9

Force Control

One of the fundamental requirements for the success of a manipulation task is the capacity to handle *interaction between manipulator and environment*. The quantity that describes the state of interaction more effectively is the *contact force* at the manipulator's end-effector. High values of contact force are generally undesirable since they may stress both the manipulator and the manipulated object. In this chapter, performance of operational space motion control schemes is studied first, during the interaction of a manipulator with the environment. The concepts of mechanical *compliance* and *impedance* are introduced, with special regard to the problem of integrating contact force measurements into the control strategy. Then, *force control* schemes are presented which are obtained from motion control schemes suitably modified by the closure of an outer force regulation feedback loop. For the planning of control actions to perform an interaction task, *natural constraints* set by the task geometry and *artificial constraints* set by the control strategy are established; the constraints are referred to a suitable constraint frame. The formulation is conveniently exploited to derive *hybrid force/motion control* schemes.

9.1 Manipulator Interaction with Environment

Control of interaction between a robot manipulator and the environment is crucial for successful execution of a number of practical tasks where the robot's end-effector has to manipulate an object or perform some operation on a surface. Typical examples include polishing, deburring, machining or assembly. A complete classification of possible robot tasks is practically infeasible in view of the large variety of cases that may occur, nor would such a classification be really useful to find a general strategy to *interaction control* with the environment.

During the interaction, the environment sets constraints on the geometric paths that can be followed by the end-effector. This situation is generally referred to as *constrained motion*. In such a case, the use of a purely motion

control strategy for controlling interaction is a candidate to fail, as explained below.

Successful execution of an interaction task with the environment by using motion control could be obtained only if the task were accurately planned. This would, in turn, require an accurate model of both the robot manipulator (kinematics and dynamics) and the environment (geometry and mechanical features). Manipulator modelling can be achieved with enough precision, but a detailed description of the environment is difficult to obtain.

To understand the importance of task planning accuracy, it is sufficient to observe that to perform a mechanical part mating with a positional approach, the relative positioning of the parts should be guaranteed with an accuracy of an order of magnitude greater than part mechanical tolerance. Once the absolute position of one part is exactly known, the manipulator should guide the motion of the other with the same accuracy.

In practice, the planning errors may give rise to a contact force causing a deviation of the end-effector from the desired trajectory. On the other hand, the control system reacts to reduce such deviation. This ultimately leads to a build-up of the contact force until saturation of the joint actuators is reached or breakage of the parts in contact occurs.

The higher the environment stiffness and position control accuracy, the more likely a situation like the one just described can occur. This drawback can be overcome if compliant behaviour is ensured during the interaction.

From the above discussion it should be clear that the *contact force* is the quantity describing the state of interaction in the most complete fashion; to this end, the availability of force measurements is expected to provide enhanced performance for controlling interaction.

Interaction control strategies can be grouped in two categories; those performing *indirect force control* and those performing *direct force control*. The main difference between the two categories is that the former achieve force control via motion control, without explicit closure of a force feedback loop; the latter, instead, offer the possibility of controlling the contact force to a desired value, thanks to the closure of a force feedback loop. To the first category belong *compliance control* and *impedance control* which are treated next. Then, *force control* and *hybrid force/motion control* schemes will follow.

9.2 Compliance Control

For a detailed analysis of interaction between the manipulator and environment it is worth considering the behaviour of the system under a position control scheme when contact forces arise. Since these are naturally described in the operational space, it is convenient to refer to *operational space control* schemes.

Consider the manipulator dynamic model (8.7). In view of (7.42), the model can be written as

$$\boldsymbol{B}(\boldsymbol{q})\ddot{\boldsymbol{q}} + \boldsymbol{C}(\boldsymbol{q},\dot{\boldsymbol{q}})\dot{\boldsymbol{q}} + \boldsymbol{F}\dot{\boldsymbol{q}} + \boldsymbol{g}(\boldsymbol{q}) = \boldsymbol{u} - \boldsymbol{J}^T(\boldsymbol{q})\boldsymbol{h}_e \tag{9.1}$$

where $\boldsymbol{h}_e$ is the vector of contact forces exerted by the manipulator's end-effector on the environment.[1]

It is reasonable to predict that, in the case $\boldsymbol{h}_e \neq \boldsymbol{0}$, the control scheme based on (8.110) no longer ensures that the end-effector reaches its desired pose $\boldsymbol{x}_d$. In fact, by recalling that $\widetilde{\boldsymbol{x}} = \boldsymbol{x}_d - \boldsymbol{x}_e$, where $\boldsymbol{x}_e$ denotes the end-effector pose, at the equilibrium it is

$$\boldsymbol{J}_A^T(\boldsymbol{q})\boldsymbol{K}_P\widetilde{\boldsymbol{x}} = \boldsymbol{J}^T(\boldsymbol{q})\boldsymbol{h}_e. \tag{9.2}$$

On the assumption of a full-rank Jacobian, one has

$$\widetilde{\boldsymbol{x}} = \boldsymbol{K}_P^{-1}\boldsymbol{T}_A^T(\boldsymbol{x}_e)\boldsymbol{h}_e = \boldsymbol{K}_P^{-1}\boldsymbol{h}_A \tag{9.3}$$

where $\boldsymbol{h}_A$ is the vector of equivalent forces that can be defined according to (7.128). The expression in (9.3) shows that at the equilibrium the manipulator, under a pose control action, behaves like a generalized spring in the operational space with *compliance* $\boldsymbol{K}_P^{-1}$ in respect of the equivalent force $\boldsymbol{h}_A$. By recalling the expression of the transformation matrix $\boldsymbol{T}_A$ in (3.65) and assuming matrix $\boldsymbol{K}_P$ to be diagonal, it can be recognized that linear compliance (due to force components) is independent of the configuration, whereas torsional compliance (due to moment components) does depend on the current end-effector orientation through the matrix $\boldsymbol{T}$.

On the other hand, if $\boldsymbol{h}_e \in \mathcal{N}(\boldsymbol{J}^T)$, one has $\widetilde{\boldsymbol{x}} = \boldsymbol{0}$ with $\boldsymbol{h}_e \neq \boldsymbol{0}$, namely contact forces are completely balanced by the manipulator mechanical structure; for instance, the anthropomorphic manipulator at a shoulder singularity in Fig. 3.13 does not react to any force orthogonal to the plane of the structure.

Equation (9.3) can be rewritten in the form

$$\boldsymbol{h}_A = \boldsymbol{K}_P\widetilde{\boldsymbol{x}} \tag{9.4}$$

where $\boldsymbol{K}_P$ represents a *stiffness* matrix as regards the vector of the equivalent forces $\boldsymbol{h}_A$. It is worth observing that the compliant (or stiff) behaviour of the manipulator is achieved by virtue of the control. This behaviour is termed *active compliance* whereas the term *passive compliance* denotes mechanical systems with a prevalent dynamics of elastic type.

For a better understanding of the interaction between manipulator and environment, it is necessary to analyze further the concept of passive compliance.

[1] In this chapter the term force, in general, is referred to a (6×1) vector of force and moment, unless otherwise specified.

9.2.1 Passive Compliance

Consider two elastically coupled rigid bodies R and S and two reference frames, each attached to one of the two bodies so that at equilibrium, in the absence of interaction forces and moments, the two frames coincide. Let $d\boldsymbol{x}_{r,s}$ denote an elementary displacement from the equilibrium of frame s with respect to frame r, defined as

$$d\boldsymbol{x}_{r,s} = \begin{bmatrix} d\boldsymbol{o}_{r,s} \\ \boldsymbol{\omega}_{r,s}dt \end{bmatrix} = \boldsymbol{v}_{r,s}dt \tag{9.5}$$

where $\boldsymbol{v}_{r,s} = \boldsymbol{v}_s - \boldsymbol{v}_r$ is the vector of linear and angular velocity of frame s with respect to frame r, $d\boldsymbol{o}_{r,s} = \boldsymbol{o}_s - \boldsymbol{o}_r$ is the vector corresponding to the translation of the origin $\boldsymbol{o}_s$ of frame s with respect to the origin $\boldsymbol{o}_r$ of frame r and $\boldsymbol{\omega}_{r,s}dt$, with $\boldsymbol{\omega}_{r,s} = \boldsymbol{\omega}_s - \boldsymbol{\omega}_r$, represents the vector of small rotations of frame s about the axes of frame r as in (3.106). This elementary displacement is assumed to be equivalently referred to frame r or s because, at the equilibrium, the two frames coincide; therefore, the reference frame was not explicitly denoted.

To the displacement $d\boldsymbol{x}_{r,s}$, coinciding with the deformation of the spring between R and S, it corresponds the elastic force

$$\boldsymbol{h}_s = \begin{bmatrix} \boldsymbol{f}_s \\ \boldsymbol{\mu}_s \end{bmatrix} = \begin{bmatrix} \boldsymbol{K}_f & \boldsymbol{K}_c \\ \boldsymbol{K}_c^T & \boldsymbol{K}_\mu \end{bmatrix} \begin{bmatrix} d\boldsymbol{o}_{r,s} \\ \boldsymbol{\omega}_{r,s}dt \end{bmatrix} = \boldsymbol{K}d\boldsymbol{x}_{r,s}, \tag{9.6}$$

applied by body S on the spring and referred equivalently to one of the two reference frames. In view of the action-reaction law, the force applied by R has the expression $\boldsymbol{h}_r = -\boldsymbol{h}_s = \boldsymbol{K}d\boldsymbol{x}_{s,r}$, being $d\boldsymbol{x}_{s,r} = -d\boldsymbol{x}_{r,s}$.

The (6×6) matrix $\boldsymbol{K}$ represents a *stiffness matrix*, which is symmetric and *positive semi-definite*. The (3×3) matrices $\boldsymbol{K}_f$ and $\boldsymbol{K}_\mu$ are known as *translational stiffness* and *rotational stiffness*, respectively. The (3×3) matrix $\boldsymbol{K}_c$ is known as *coupling stiffness*. An analogous decomposition can be made for the *compliance matrix* $\boldsymbol{C}$ in the mapping

$$d\boldsymbol{x}_{r,s} = \boldsymbol{C}\boldsymbol{h}_s. \tag{9.7}$$

In the real elastic systems, matrix $\boldsymbol{K}_c$ is, in general, non-symmetric. However, there are special devices, such as the RCC (*Remote Centre of Compliance*), where $\boldsymbol{K}_c$ can be symmetric or null. These are elastically compliant mechanical devices, suitably designed to achieve maximum decoupling between translation and rotation, that are interposed between the manipulator last link and the end-effector. The aim is that of introducing a *passive compliance* of desired value to facilitate the execution of assembly tasks. For instance, in a peg-in-hole insertion task, the gripper is provided with a device ensuring high stiffness along the insertion direction and high compliance along the other directions. Therefore, in the presence of unavoidable position displacements

from the planned insertion trajectory, contact forces and moments arise which modify the peg position so as to facilitate insertion.

The inconvenience of such devices is their low versatility to different operating conditions and generic interaction tasks, namely, whenever a modification of the compliant mechanical hardware is required.

9.2.2 Active Compliance

The aim of *compliance control* is that of achieving a suitable *active compliance* that can be easily modified acting on the control software so as to satisfy the requirements of different interaction tasks.

Notice that the equilibrium equations in (9.3) and (9.4) show that the compliant behaviour with respect to $\boldsymbol{h}_e$ depends on the actual end-effector orientation, also for elementary displacements, so that, in practice, the selection of stiffness parameters is quite difficult. To obtain an equilibrium equation of the form (9.6), a different definition of error in the operational space must be considered.

Let O_e–$x_e y_e z_e$ and O_d–$x_d y_d z_d$ denote the end-effector frame and the desired frame respectively. The corresponding homogeneous transformation matrices are

$$\boldsymbol{T}_e = \begin{bmatrix} \boldsymbol{R}_e & \boldsymbol{o}_e \\ \boldsymbol{0}^T & 1 \end{bmatrix} \qquad \boldsymbol{T}_d = \begin{bmatrix} \boldsymbol{R}_d & \boldsymbol{o}_d \\ \boldsymbol{0}^T & 1 \end{bmatrix},$$

with obvious meaning of notation. The position and orientation displacement of the end-effector frame with respect to the desired frame can be expressed in terms of the homogeneous transformation matrix

$$\boldsymbol{T}_e^d = (\boldsymbol{T}_d)^{-1}\boldsymbol{T}_e = \begin{bmatrix} \boldsymbol{R}_e^d & \boldsymbol{o}_{d,e}^d \\ \boldsymbol{0}^T & 1 \end{bmatrix}, \tag{9.8}$$

where $\boldsymbol{R}_e^d = \boldsymbol{R}_d^T \boldsymbol{R}_e$ and $\boldsymbol{o}_{d,e}^d = \boldsymbol{R}_d^T(\boldsymbol{o}_e - \boldsymbol{o}_d)$. The new error vector in the operational space can be defined as

$$\widetilde{\boldsymbol{x}} = -\begin{bmatrix} \boldsymbol{o}_{d,e}^d, \\ \boldsymbol{\phi}_{d,e} \end{bmatrix} \tag{9.9}$$

where $\boldsymbol{\phi}_{d,e}$ is the vector of Euler angles extracted from the rotation matrix $\boldsymbol{R}_e^d$. The minus sign in (9.9) depends on the fact that, for control purposes, the error is usually defined as the difference between the desired and the measured quantities.

Computing the time derivative of $\boldsymbol{o}_{d,e}^d$ and taking into account (3.10), (3.11) gives

$$\dot{\boldsymbol{o}}_{d,e}^d = \boldsymbol{R}_d^T(\dot{\boldsymbol{o}}_e - \dot{\boldsymbol{o}}_d) - \boldsymbol{S}(\boldsymbol{\omega}_d^d)\boldsymbol{R}_d^T(\boldsymbol{o}_e - \boldsymbol{o}_d). \tag{9.10}$$

On the other hand, computing the time derivative of $\boldsymbol{\phi}_{d,e}$ and taking into account (3.64), yields (see Problem 9.1)

$$\dot{\boldsymbol{\phi}}_{d,e} = \boldsymbol{T}^{-1}(\boldsymbol{\phi}_{d,e})\boldsymbol{\omega}_{d,e}^d = \boldsymbol{T}^{-1}(\boldsymbol{\phi}_{d,e})\boldsymbol{R}_d^T(\boldsymbol{\omega}_e - \boldsymbol{\omega}_d). \tag{9.11}$$

Considering that the desired quantities $\boldsymbol{o}_d$ and $\boldsymbol{R}_d$ are constant, vector $\dot{\widetilde{\boldsymbol{x}}}$ can be expressed in the form

$$\dot{\widetilde{\boldsymbol{x}}} = -\boldsymbol{T}_A^{-1}(\boldsymbol{\phi}_{d,e}) \begin{bmatrix} \boldsymbol{R}_d^T & \boldsymbol{O} \\ \boldsymbol{O} & \boldsymbol{R}_d^T \end{bmatrix} \boldsymbol{v}_e \tag{9.12}$$

being $\boldsymbol{v}_e = [\, \dot{\boldsymbol{o}}_e^T \quad \boldsymbol{\omega}_e^T \,]^T = \boldsymbol{J}(\boldsymbol{q})\dot{\boldsymbol{q}}$ the vector of linear and angular velocity of the end-effector. Therefore

$$\dot{\widetilde{\boldsymbol{x}}} = -\boldsymbol{J}_{A_d}(\boldsymbol{q}, \widetilde{\boldsymbol{x}})\dot{\boldsymbol{q}}, \tag{9.13}$$

where the matrix

$$\boldsymbol{J}_{A_d}(\boldsymbol{q}, \widetilde{\boldsymbol{x}}) = \boldsymbol{T}_A^{-1}(\boldsymbol{\phi}_{d,e}) \begin{bmatrix} \boldsymbol{R}_d^T & \boldsymbol{O} \\ \boldsymbol{O} & \boldsymbol{R}_d^T \end{bmatrix} \boldsymbol{J}(\boldsymbol{q}) \tag{9.14}$$

represents the analytical Jacobian corresponding to the definition (9.9) of error in the operational space.

The PD control with gravity compensation analogous to (8.110), with the definition (9.9) of error in the operational space, has the expression

$$\boldsymbol{u} = \boldsymbol{g}(\boldsymbol{q}) + \boldsymbol{J}_{A_d}^T(\boldsymbol{q}, \widetilde{\boldsymbol{x}})(\boldsymbol{K}_P\widetilde{\boldsymbol{x}} - \boldsymbol{K}_D\boldsymbol{J}_{A_d}(\boldsymbol{q}, \widetilde{\boldsymbol{x}})\dot{\boldsymbol{q}}). \tag{9.15}$$

Notice that, in the case where the operational space is defined only by the position components, the control laws (8.110) and (9.15) differ only because the position error (and the corresponding derivative term) is referred to the base frame in (8.110), while it is referred to the desired frame in (9.15).

In the absence of interaction, the asymptotic stability of the equilibrium pose corresponding to $\widetilde{\boldsymbol{x}} = \boldsymbol{0}$, assuming that $\boldsymbol{K}_P$ and $\boldsymbol{K}_D$ are symmetric and positive definite matrices, can be proven using the Lyapunov function

$$\boldsymbol{V}(\dot{\boldsymbol{q}}, \widetilde{\boldsymbol{x}}) = \frac{1}{2}\dot{\boldsymbol{q}}^T\boldsymbol{B}(\boldsymbol{q})\dot{\boldsymbol{q}} + \frac{1}{2}\widetilde{\boldsymbol{x}}^T\boldsymbol{K}_P\widetilde{\boldsymbol{x}} > 0 \qquad \forall \dot{\boldsymbol{q}}, \widetilde{\boldsymbol{x}} \neq \boldsymbol{0},$$

as for the case of the control law (8.110).

In the presence of interaction with the environment, at the equilibrium it is

$$\boldsymbol{J}_{A_d}^T(\boldsymbol{q})\boldsymbol{K}_P\widetilde{\boldsymbol{x}} = \boldsymbol{J}^T(\boldsymbol{q})\boldsymbol{h}_e; \tag{9.16}$$

hence, assuming a full-rank Jacobian, the following equality holds:

$$\boldsymbol{h}_e^d = \boldsymbol{T}_A^{-T}(\boldsymbol{\phi}_{d,e})\boldsymbol{K}_P\widetilde{\boldsymbol{x}}. \tag{9.17}$$

The above equation, to be compared to the elastic model (9.6), must be rewritten in terms of elementary displacements. To this end, taking into account (9.12) and (9.5), it is

$$d\widetilde{\boldsymbol{x}} = \dot{\widetilde{\boldsymbol{x}}}\Big|_{\widetilde{\boldsymbol{x}}=\boldsymbol{0}} dt = \boldsymbol{T}_A^{-1}(\boldsymbol{0})(\boldsymbol{v}_d^d - \boldsymbol{v}_e^d)dt = \boldsymbol{T}_A^{-1}(\boldsymbol{0})d\boldsymbol{x}_{e,d} \tag{9.18}$$

where $d\boldsymbol{x}_{e,d}$ is the elementary displacement of the desired frame with respect to the end-effector frame about the equilibrium, referred to any of the two frames. The value of $\boldsymbol{T}_A(\boldsymbol{0})$ depends on the particular choice of Euler angles; in the following, angles XYZ are adopted, for which $\boldsymbol{T}_A(\boldsymbol{0}) = \boldsymbol{I}$ (see Problem 3.13). Therefore, rewriting (9.17) in terms of elementary displacements gives

$$\boldsymbol{h}_e = \boldsymbol{K}_P d\boldsymbol{x}_{e,d}, \tag{9.19}$$

which is formally identical to (9.6), where vectors are assumed to be referred to the desired frame or to the end-effector frame, equivalently. It follows that matrix $\boldsymbol{K}_P$ has the meaning of an active stiffness corresponding to a generalized spring acting between the end-effector frame and the desired frame. Equation (9.19) can be rewritten in the equivalent form

$$d\boldsymbol{x}_{e,d} = \boldsymbol{K}_P^{-1} \boldsymbol{h}_e, \tag{9.20}$$

showing that $\boldsymbol{K}_P^{-1}$ corresponds to an active compliance.

The selection of the elements of matrix $\boldsymbol{K}_P$ must be made taking into account geometry and mechanical features of the environment. To this end, assume that the interaction force between the end-effector and the environment derives from a generalized spring acting between the end-effector frame and a reference frame O_r–$x_r y_r z_r$ attached to the environment rest position. Considering an elementary displacement $d\boldsymbol{x}_{r,e}$ between the two reference frames, the corresponding elastic force applied by the end-effector is

$$\boldsymbol{h}_e = \boldsymbol{K} d\boldsymbol{x}_{r,e} \tag{9.21}$$

with a stiffness matrix $\boldsymbol{K}$, where vectors can be referred, equivalently, to the frame attached to the rest position of the environment or to the end-effector frame. Typically, the stiffness matrix is positive semi-definite because, in general, the interaction forces and moments belong to some particular directions, spanning $\mathcal{R}(\boldsymbol{K})$.

In view of the model (9.21), of (9.19) and of the equality

$$d\boldsymbol{x}_{r,e} = d\boldsymbol{x}_{r,d} - d\boldsymbol{x}_{e,d},$$

the following expression of the contact force at equilibrium can be found:

$$\boldsymbol{h}_e = \left(\boldsymbol{I}_6 + \boldsymbol{K}\boldsymbol{K}_P^{-1}\right)^{-1} \boldsymbol{K} d\boldsymbol{x}_{r,d}. \tag{9.22}$$

Substituting this expression into (9.20) yields

$$d\boldsymbol{x}_{e,d} = \boldsymbol{K}_P^{-1}\left(\boldsymbol{I}_6 + \boldsymbol{K}\boldsymbol{K}_P^{-1}\right)^{-1} \boldsymbol{K} d\boldsymbol{x}_{r,d}, \tag{9.23}$$

representing the pose error of the end-effector at the equilibrium.

Notice that vectors in (9.22) and (9.23) can be referred, equivalently, to the end-effector frame, to the desired frame or to the frame attached to the environment rest position; these frames coincide at equilibrium (see Problem 9.2).

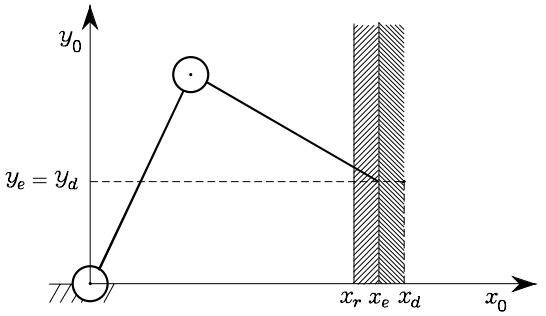

Fig. 9.1. Two-link planar arm in contact with an elastically compliant plane

The analysis of (9.23) shows that the end-effector pose error at the equilibrium depends on the environment rest position, as well as on the desired pose imposed by the control system of the manipulator. The interaction of the two systems (environment and manipulator) is influenced by the mutual weight of the respective compliance features.

In fact, it is possible to modify the active compliance $\boldsymbol{K}_P^{-1}$ so that the manipulator dominates the environment and vice versa. Such a dominance can be specified with reference to the single directions of the operational space.

For a given environment stiffness $\boldsymbol{K}$, according to the prescribed interaction task, one may choose large values of the elements of $\boldsymbol{K}_P$ for those directions along which the environment has to comply and small values of the elements of $\boldsymbol{K}_P$ for those directions along which the manipulator has to comply. As a consequence, the manipulator pose error $d\boldsymbol{x}_{e,d}$ tends to zero along the directions where the environment complies; vice versa, along the directions where the manipulator complies, the end-effector pose tends to the rest pose of the environment, namely $d\boldsymbol{x}_{e,d} \simeq d\boldsymbol{x}_{r,d}$.

Equation (9.22) gives the value of the contact force at the equilibrium. This expression reveals that, along the directions where the manipulator stiffness is much higher than the environment stiffness, the intensity of the elastic force mainly depends on the stiffness of the environment and on the displacement $d\boldsymbol{x}_{r,e}$ between the equilibrium pose of the end-effector (which practically coincides with the desired pose) and the rest pose of the environment. In the dual case that the environment stiffness is much higher than the manipulator stiffness, the intensity of the elastic force mainly depends on the manipulator stiffness and on the displacement $d\boldsymbol{x}_{e,d}$ between the desired pose and the equilibrium pose of the end-effector (which practically coincides with the rest pose of the environment).

Example 9.1

Consider the two-link planar arm whose tip is in contact with a purely frictionless elastic plane; due to the simple geometry of the problem, involving only position variables, all the quantities can be conveniently referred to the base frame. Thus, control law (8.110) will be adopted. Let $\boldsymbol{o}_r = [\, x_r \quad 0 \,]^T$ denote the equilibrium position of the plane, which is assumed to be orthogonal to axis x_0 (Fig. 9.1). The environment stiffness matrix is

$$\boldsymbol{K} = \boldsymbol{K}_f = \mathrm{diag}\{k_x, 0\},$$

corresponding to the absence of interaction forces along the vertical direction ($\boldsymbol{f}_e = [\, f_x \quad 0 \,]^T$). Let $\boldsymbol{o}_e = [\, x_e \quad y_e \,]^T$ be the end-effector position and $\boldsymbol{o}_d = [\, x_d \quad y_d \,]^T$ be the desired position, which is located beyond the contact plane. The proportional control action on the arm is characterized by

$$\boldsymbol{K}_P = \mathrm{diag}\{k_{Px}, k_{Py}\}.$$

The equilibrium equations for the force and position (9.22), (9.23), rewritten with $d\boldsymbol{x}_{r,d} = \boldsymbol{o}_d - \boldsymbol{o}_r$ and $d\boldsymbol{x}_{e,d} = \boldsymbol{o}_d - \boldsymbol{o}_e$, give

$$\boldsymbol{f}_e = \begin{bmatrix} \dfrac{k_{Px}k_x}{k_{Px}+k_x}(x_d - x_r) \\ 0 \end{bmatrix} \qquad \boldsymbol{o}_e = \begin{bmatrix} \dfrac{k_{Px}x_d + k_x x_r}{k_{Px}+k_x} \\ y_d \end{bmatrix}.$$

With reference to positioning accuracy, the arm tip reaches the vertical coordinate y_d, since the vertical motion direction is not constrained. As for the horizontal direction, the presence of the elastic plane imposes that the arm can move as far as it reaches the coordinate $x_e < x_d$. The value of the horizontal contact force at the equilibrium is related to the difference between x_d and x_r by an equivalent stiffness coefficient which is given by the parallel composition of the stiffness coefficients of the two interacting systems. Hence, the arm stiffness and environment stiffness influence the resulting equilibrium configuration. In the case when

$$k_{Px}/k_x \gg 1,$$

it is

$$x_e \approx x_d \qquad f_x \approx k_x(x_d - x_r)$$

and thus the arm prevails over the environment, in that the plane complies almost up to x_d and the elastic force is mainly generated by the environment (passive compliance). In the opposite case

$$k_{Px}/k_x \ll 1,$$

it is

$$x_e \approx x_r \qquad f_x \approx k_{Px}(x_d - x_r)$$

and thus the environment prevails over the arm which complies up to the equilibrium x_r, and the elastic force is mainly generated by the arm (active compliance).

To complete the analysis of manipulator compliance in contact with environment, it is worth considering the effects of a joint space position control law. With reference to (8.51), in the presence of end-effector contact forces, the equilibrium posture is determined by

$$\boldsymbol{K}_P\widetilde{\boldsymbol{q}} = \boldsymbol{J}^T(\boldsymbol{q})\boldsymbol{h}_e \tag{9.24}$$

and then

$$\widetilde{\boldsymbol{q}} = \boldsymbol{K}_P^{-1}\boldsymbol{J}^T(\boldsymbol{q})\boldsymbol{h}_e. \tag{9.25}$$

On the assumption of small displacements from the equilibrium, it is reasonable to compute the resulting operational space displacement as $d\widetilde{\boldsymbol{x}} \approx \boldsymbol{J}(\boldsymbol{q})d\widetilde{\boldsymbol{q}}$, referred to the base frame. Therefore, in view of (9.25) it is

$$d\widetilde{\boldsymbol{x}} = \boldsymbol{J}(\boldsymbol{q})\boldsymbol{K}_P^{-1}\boldsymbol{J}^T(\boldsymbol{q})\boldsymbol{h}_e, \tag{9.26}$$

corresponding to an active compliance referred to the base frame. Notice that the compliance matrix $\boldsymbol{J}(\boldsymbol{q})\boldsymbol{K}_P^{-1}\boldsymbol{J}^T(\boldsymbol{q})$ depends on the manipulator posture, both for the force and moment components. Also in this case, the occurrence of manipulator Jacobian singularities is to be analyzed apart.

9.3 Impedance Control

It is now desired to analyze the interaction of a manipulator with the environment under the action of an inverse dynamics control in the operational space. With reference to model (9.1), consider the control law (8.57)

$$\boldsymbol{u} = \boldsymbol{B}(\boldsymbol{q})\boldsymbol{y} + \boldsymbol{n}(\boldsymbol{q}, \dot{\boldsymbol{q}}),$$

with $\boldsymbol{n}$ as in (8.56). In the presence of end-effector forces, the controlled manipulator is described by

$$\ddot{\boldsymbol{q}} = \boldsymbol{y} - \boldsymbol{B}^{-1}(\boldsymbol{q})\boldsymbol{J}^T(\boldsymbol{q})\boldsymbol{h}_e \tag{9.27}$$

that reveals the existence of a nonlinear coupling term due to contact forces. Choose $\boldsymbol{y}$ in a way conceptually analogous to (8.114), as

$$\boldsymbol{y} = \boldsymbol{J}_A^{-1}(\boldsymbol{q})\boldsymbol{M}_d^{-1}\big(\boldsymbol{M}_d\ddot{\boldsymbol{x}}_d + \boldsymbol{K}_D\dot{\widetilde{\boldsymbol{x}}} + \boldsymbol{K}_P\widetilde{\boldsymbol{x}} - \boldsymbol{M}_d\dot{\boldsymbol{J}}_A(\boldsymbol{q}, \dot{\boldsymbol{q}})\dot{\boldsymbol{q}}\big) \tag{9.28}$$

where $\boldsymbol{M}_d$ is a positive definite diagonal matrix. Substituting (9.28) into (9.27) and accounting for second-order differential kinematics in the form (3.98), yields

$$\boldsymbol{M}_d\ddot{\widetilde{\boldsymbol{x}}} + \boldsymbol{K}_D\dot{\widetilde{\boldsymbol{x}}} + \boldsymbol{K}_P\widetilde{\boldsymbol{x}} = \boldsymbol{M}_d\boldsymbol{B}_A^{-1}(\boldsymbol{q})\boldsymbol{h}_A, \tag{9.29}$$

where

$$\boldsymbol{B}_A(\boldsymbol{q}) = \boldsymbol{J}_A^{-T}(\boldsymbol{q})\boldsymbol{B}(\boldsymbol{q})\boldsymbol{J}_A^{-1}(\boldsymbol{q})$$

is the inertia matrix of the manipulator in the operational space as in (7.134); this matrix is configuration-dependent and is positive definite if $\boldsymbol{J}_A$ has full rank.

The expression in (9.29) establishes a relationship through a generalized *mechanical impedance* between the vector of forces $\boldsymbol{M}_d\boldsymbol{B}_A^{-1}\boldsymbol{h}_A$ and the vector of displacements $\widetilde{\boldsymbol{x}}$ in the operational space. This impedance can be attributed to a mechanical system characterized by a mass matrix $\boldsymbol{M}_d$, a damping matrix $\boldsymbol{K}_D$, and a stiffness matrix $\boldsymbol{K}_P$, which can be used to specify the dynamic behaviour along the operational space directions.

The presence of $\boldsymbol{B}_A^{-1}$ makes the system coupled. If it is wished to keep linearity and decoupling during interaction with the environment, it is then necessary to *measure* the contact *force*; this can be achieved by means of appropriate force sensors which are usually mounted to the manipulator wrist, as discussed in Sect. 5.4.1. Choosing

$$\boldsymbol{u} = \boldsymbol{B}(\boldsymbol{q})\boldsymbol{y} + \boldsymbol{n}(\boldsymbol{q}, \dot{\boldsymbol{q}}) + \boldsymbol{J}^T(\boldsymbol{q})\boldsymbol{h}_e \tag{9.30}$$

with

$$\boldsymbol{y} = \boldsymbol{J}_A^{-1}(\boldsymbol{q})\boldsymbol{M}_d^{-1}\big(\boldsymbol{M}_d\ddot{\boldsymbol{x}}_d + \boldsymbol{K}_D\dot{\widetilde{\boldsymbol{x}}} + \boldsymbol{K}_P\widetilde{\boldsymbol{x}} - \boldsymbol{M}_d\dot{\boldsymbol{J}}_A(\boldsymbol{q}, \dot{\boldsymbol{q}})\dot{\boldsymbol{q}} - \boldsymbol{h}_A\big), \tag{9.31}$$

under the assumption of error-free force measurements, yields

$$\boldsymbol{M}_d\ddot{\widetilde{\boldsymbol{x}}} + \boldsymbol{K}_D\dot{\widetilde{\boldsymbol{x}}} + \boldsymbol{K}_P\widetilde{\boldsymbol{x}} = \boldsymbol{h}_A. \tag{9.32}$$

It is worth noticing that the addition of the term $\boldsymbol{J}^T\boldsymbol{h}_e$ in (9.30) exactly compensates the contact forces and then it renders the manipulator infinitely stiff as regards the external stress. In order to confer a compliant behaviour to the manipulator, the term $-\boldsymbol{J}_A^{-1}\boldsymbol{M}_d^{-1}\boldsymbol{h}_A$ has been introduced in (9.31) so that the manipulator can be characterized as a *linear impedance* with regard to the equivalent forces $\boldsymbol{h}_A$, as shown in (9.32).

The behaviour of the system in (9.32) at the equilibrium is analogous to that described by (9.4); nonetheless, compared to a control with active compliance specified by $\boldsymbol{K}_P^{-1}$, the equation in (9.32) allows a complete characterization of system dynamics through an *active impedance* specified by matrices $\boldsymbol{M}_d$, $\boldsymbol{K}_D$, $\boldsymbol{K}_P$. Also in this case, it is not difficult to recognize that, as regards $\boldsymbol{h}_e$, impedance depends on the current end-effector orientation through the matrix $\boldsymbol{T}$. Therefore, the selection of the impedance parameters becomes difficult; moreover, an inadequate behaviour may occur in the neighbourhood of representation singularities.

To avoid this problem it is sufficient to redesign the control input $\boldsymbol{y}$ as a function of the operational space error (9.9).

Under the assumption that the desired frame O_d–$x_dy_dz_d$ is time-varying, in view of (9.10), (9.11), the time derivative of (9.9) has the expression

$$\dot{\widetilde{\boldsymbol{x}}} = -\boldsymbol{J}_{A_d}(\boldsymbol{q}, \widetilde{\boldsymbol{x}})\dot{\boldsymbol{q}} + \boldsymbol{b}(\widetilde{\boldsymbol{x}}, \boldsymbol{R}_d, \dot{\boldsymbol{o}}_d, \boldsymbol{\omega}_d), \tag{9.33}$$

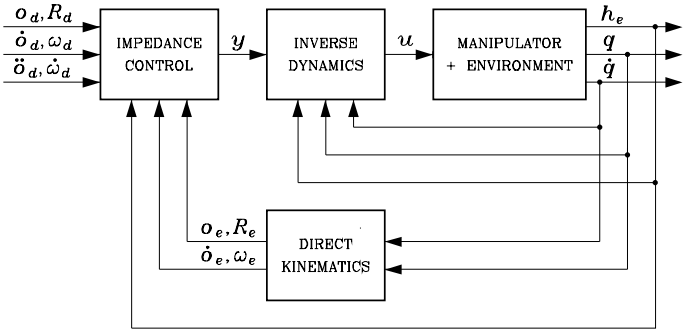

Fig. 9.2. Block scheme of impedance control

where $\boldsymbol{J}_{A_d}$ is the analytical Jacobian (9.14) and vector $\boldsymbol{b}$ is

$$\boldsymbol{b}(\widetilde{\boldsymbol{x}}, \boldsymbol{R}_d, \dot{\boldsymbol{o}}_d, \boldsymbol{\omega}_d) = \begin{bmatrix} \boldsymbol{R}_d^T \dot{\boldsymbol{o}}_d + \boldsymbol{S}(\omega_d^d)\boldsymbol{o}_{d,e}^d \\ \boldsymbol{T}^{-1}(\boldsymbol{\phi}_{d,e})\boldsymbol{\omega}_d^d \end{bmatrix}.$$

Computing the time derivative of (9.33) yields

$$\dddot{\widetilde{\boldsymbol{x}}} = -\boldsymbol{J}_{A_d}\ddot{\boldsymbol{q}} - \dot{\boldsymbol{J}}_{A_d}\dot{\boldsymbol{q}} + \dot{\boldsymbol{b}}, \tag{9.34}$$

where, for simplicity, the dependence of the functions on their arguments was omitted. As a consequence, using (9.30) with

$$\boldsymbol{y} = \boldsymbol{J}_{A_d}^{-1}\boldsymbol{M}_d^{-1}\big(\boldsymbol{K}_D\ddot{\widetilde{\boldsymbol{x}}} + \boldsymbol{K}_P\dot{\widetilde{\boldsymbol{x}}} - \boldsymbol{M}_d\dot{\boldsymbol{J}}_{A_d}\dot{\boldsymbol{q}} + \boldsymbol{M}_d\dot{\boldsymbol{b}} - \boldsymbol{h}_e^d\big), \tag{9.35}$$

yields the equation

$$\boldsymbol{M}_d\dddot{\widetilde{\boldsymbol{x}}} + \boldsymbol{K}_D\ddot{\widetilde{\boldsymbol{x}}} + \boldsymbol{K}_P\dot{\widetilde{\boldsymbol{x}}} = \boldsymbol{h}_e^d, \tag{9.36}$$

where all the vectors are referred to the desired frame. This equation represents a linear impedance as regards the force vector $\boldsymbol{h}_e^d$, independent from the manipulator configuration.

The block scheme representing impedance control is reported in Fig. 9.2.

Similar to active and passive compliance, the concept of *passive impedance* can be introduced if the interaction force $\boldsymbol{h}_e$ is generated at the contact with an environment of proper mass, damping and stiffness. In this case, the system of manipulator with environment can be regarded as a mechanical system constituted by the parallel of the two impedances, and then its dynamic behaviour is conditioned by the relative weight between them.

Example 9.2

Consider the planar arm in contact with an elastically compliant plane of the previous example. Due to the simple geometry of the problem, involving only position

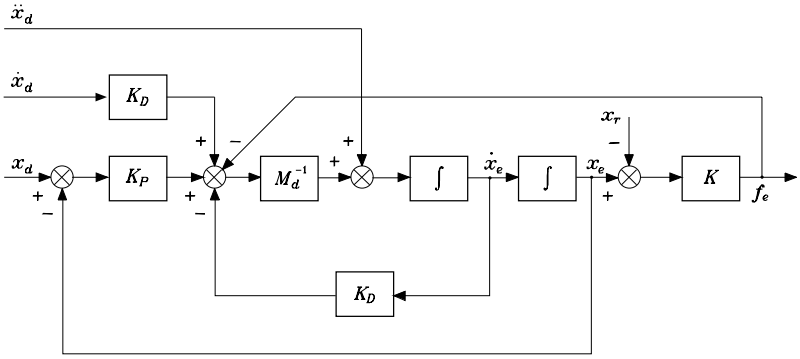

Fig. 9.3. Equivalent block scheme of a manipulator in contact with an elastic environment under impedance control

variables, all the quantities can be conveniently referred to the base frame. Thus, the impedance control law with force measurement (9.30), (9.31) will be adopted. Moreover, $\boldsymbol{x}_d = \boldsymbol{o}_d$, $\widetilde{\boldsymbol{x}} = \boldsymbol{o}_d - \boldsymbol{o}_e$, $\boldsymbol{h}_A = \boldsymbol{f}_e$ and

$$\boldsymbol{M}_d = \mathrm{diag}\{m_{dx}, m_{dy}\} \qquad \boldsymbol{K}_D = \mathrm{diag}\{k_{Dx}, k_{Dy}\} \qquad \boldsymbol{K}_P = \mathrm{diag}\{k_{Px}, k_{Py}\}.$$

The block scheme of the manipulator in contact with an elastic environment under impedance control is represented in Fig. 9.3, where $\boldsymbol{x}_e = \boldsymbol{o}_e$ and $\boldsymbol{x}_r = \boldsymbol{o}_r$.

If $\boldsymbol{x}_d$ is constant, the dynamics of the manipulator and environment system along the two directions of the operational space is described by

$$\begin{aligned} m_{dx}\ddot{x}_e + k_{Dx}\dot{x}_e + (k_{Px} + k_x)x_e &= k_x x_r + k_{Px} x_d \\ m_{dy}\ddot{y}_e + k_{Dy}\dot{y}_e + k_{Py} y_e &= k_{Py} y_d. \end{aligned}$$

Along the vertical direction, one has an unconstrained motion whose time behaviour is determined by the following natural frequency and damping factor:

$$\omega_{ny} = \sqrt{\frac{k_{Py}}{m_{dy}}} \qquad \zeta_y = \frac{k_{Dy}}{2\sqrt{m_{dy} k_{Py}}},$$

while, along the horizontal direction, the behaviour of the contact force $f_x = k_x(x_e - x_r)$ is determined by

$$\omega_{nx} = \sqrt{\frac{k_{Px} + k_x}{m_{dx}}} \qquad \zeta_x = \frac{k_{Dx}}{2\sqrt{m_{dx}(k_{Px} + k_x)}}.$$

Below, the dynamic behaviour of the system is analyzed for two different values of environment compliance: $k_x = 10^3$ N/m and $k_x = 10^4$ N/m. The rest position of the environment is $x_r = 1$. The actual arm is the same as in Example 7.2. Apply an impedance control with force measurement of the kind (9.30), (9.31), and PD control actions equivalent to those chosen in the simulations of Sect. 8.7, namely

$$m_{dx} = m_{dy} = 100 \qquad k_{Dx} = k_{Dy} = 500 \qquad k_{Px} = k_{Py} = 2500.$$

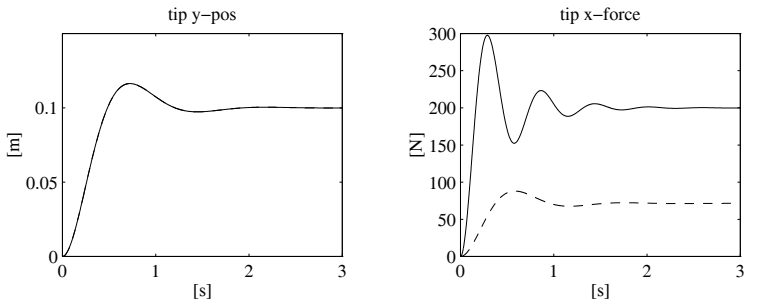

Fig. 9.4. Time history of the tip position along vertical direction and of the contact force along horizontal direction with impedance control scheme for environments of different compliance

For these values it is

$$\omega_{ny} = 5\,\text{rad/s} \qquad \zeta_y = 0.5.$$

Then, for the more compliant environment it is

$$\omega_{nx} \approx 5.9\,\text{rad/s} \qquad \zeta_x \approx 0.42$$

whereas for the less compliant environment it is

$$\omega_{nx} \approx 11.2\,\text{rad/s} \qquad \zeta_x \approx 0.22.$$

Let the arm tip be in contact with the environment at position $\boldsymbol{x}_e = [\,1 \quad 0\,]^T$; it is desired to take it to position $\boldsymbol{x}_d = [\,1.1 \quad 0.1\,]^T$.

The results in Fig. 9.4 show that motion dynamics along the vertical direction is the same in the two cases. As regards the contact force along the horizontal direction, for the more compliant environment (*dashed line*) a well-damped behaviour is obtained, whereas for the less compliant environment (*solid line*) the resulting behaviour is less damped. Further, at the equilibrium, in the first case a displacement of 7.14 cm with a contact force of 71.4 N, whereas in the second case a displacement of 2 cm with a contact force of 200 N are observed.

The selection of good impedance parameters, so as to achieve a satisfactory behaviour during the interaction, is not an easy task. Example 9.2 showed that the closed-loop dynamics along the free motion directions is different from the closed-loop dynamics along the constrained directions. In this latter case, the dynamic behaviour depends on the stiffness characteristics of the environment. The execution of a complex task, involving different types of interaction, may require different values of impedance parameters.

Notice that impedance control, in the absence of interaction or along the directions of free motion, is equivalent to an inverse dynamics position control. Therefore, for the selection of the impedance parameters, one also has to take into account the need to ensure high values to the rejection factor of the disturbances due to model uncertainties and to the approximations into the

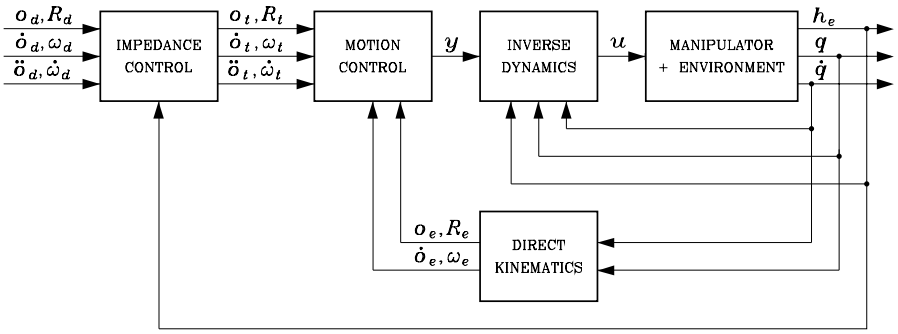

Fig. 9.5. Block scheme of admittance control

inverse dynamics computation. Such a factor increases proportionally to the gain matrix $\boldsymbol{K}_P$. Hence the closed-loop behaviour is the more degraded by disturbances, the more compliant the impedance control is made (by choosing low values for the elements of $\boldsymbol{K}_P$) to keep interaction forces limited.

A possible solution may be that of separating the motion control problem from the impedance control problem according to the control scheme represented in Fig. 9.5. The scheme is based on the concept of *compliant frame*, which is a suitable reference frame describing the ideal behaviour of the end-effector under impedance control. This frame is specified by the position of the origin $\boldsymbol{o}_t$, the rotation matrix $\boldsymbol{R}_t$, as well as by the liner and angular velocities and accelerations. These quantities can be computed by integrating the impedance equations in the form

$$\boldsymbol{M}_t \ddot{\widetilde{\boldsymbol{z}}} + \boldsymbol{K}_{Dt} \dot{\widetilde{\boldsymbol{z}}} + \boldsymbol{K}_{Pt} \widetilde{\boldsymbol{z}} = \boldsymbol{h}_e^d, \tag{9.37}$$

starting from the measurements of the force vector $\boldsymbol{h}_e$, where $\boldsymbol{M}_t$, $\boldsymbol{K}_{Dt}$, $\boldsymbol{K}_{Pt}$ are the parameters of a mechanical impedance. In the above equation, vector $\widetilde{\boldsymbol{z}}$ represents the operational space error between the desired frame and the compliant frame, as defined in (9.9), using subscript t in place of subscript e.

The kinematic variables of the compliant frame are then input to the motion control of inverse dynamics type, computed according to Eqs. (9.28), (9.30). In this way, the gains of the motion control law (9.28) can be designed so as to guarantee a high value of the disturbance rejection factor. On the other hand, the gains of the impedance control law (9.37) can be set so as to guarantee satisfactory behaviour during the interaction with the environment. Stability of the overall system can be ensured provided that the equivalent bandwidth of the motion control loop is larger than the equivalent bandwidth of the impedance control loop.

The above control scheme is also known as *admittance control* because Equation (9.37) corresponds to a mechanical admittance being used by the controller to generate the motion variables (outputs) from the force measurements (inputs). On the other hand, the control defined by Eqs. (9.31) or (9.35)

and (9.30) can be interpreted as a system producing equivalent end-effector forces (outputs) from the measurements of the motion variables (inputs), thus corresponding to a mechanical impedance.

9.4 Force Control

The above schemes implement an *indirect force control*, because the interaction force can be indirectly controlled by acting on the desired pose of the end-effector assigned to the motion control system. Interaction between manipulator and environment is anyhow directly influenced by compliance of the environment and by either compliance or impedance of the manipulator.

If it is desired to control accurately the contact force, it is necessary to devise control schemes that allow the desired interaction force to be directly specified. The development of a *direct force control* system, in analogy to a motion control system, would require the adoption of a stabilizing PD control action on the force error besides the usual nonlinear compensation actions. Force measurements may be corrupted by noise, and then a derivative action may not be implemented in practice. The stabilizing action is to be provided by suitable damping of velocity terms. As a consequence, a force control system typically features a control law based not only on force measurements but also on velocity measurements, and eventually position measurements too.

The realization of a force control scheme can be entrusted to the closure of an *outer force regulation feedback loop* generating the control input for the motion control scheme the manipulator is usually endowed with. Therefore, force control schemes are presented below, which are based on the use of an inverse dynamics position control. The effectiveness of a such control scheme depends on the particular interaction cases and, in general, on the contact geometry. To this end, notice that a force control strategy is meaningful only for those directions of the operational space along which interaction forces between manipulator and environment may arise.

Below, force control schemes based on the adoption of motion control laws of inverse dynamics type are presented, assuming that the operational space is defined only by position variables. Therefore, the end-effector pose can be specified by the operational space vector $\boldsymbol{x}_e = \boldsymbol{o}_e$. Moreover, the elastic model

$$\boldsymbol{f}_e = \boldsymbol{K}(\boldsymbol{x}_e - \boldsymbol{x}_r) \tag{9.38}$$

is assumed for the environment, obtained from (9.21) with the assumption that only forces arise at the contact. In (9.38), consider $\boldsymbol{x}_r = \boldsymbol{o}_r$ and assume that the axes of the frame attached to the environment rest position are parallel to the axes of the base frame. The above assumptions allow some important features of force control to be evidenced.

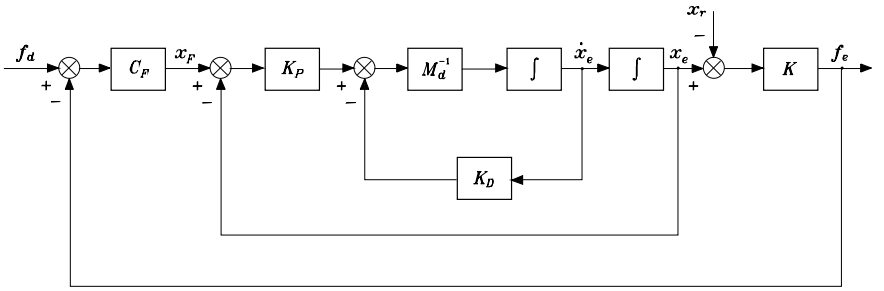

Fig. 9.6. Block scheme of force control with inner position loop

9.4.1 Force Control with Inner Position Loop

With reference to the inverse dynamics law with force measurement (9.30), choose in place of (9.31), the control

$$\boldsymbol{y} = \boldsymbol{J}^{-1}(\boldsymbol{q})\boldsymbol{M}_d^{-1}\big(-\boldsymbol{K}_D\dot{\boldsymbol{x}}_e + \boldsymbol{K}_P(\boldsymbol{x}_F - \boldsymbol{x}_e) - \boldsymbol{M}_d\dot{\boldsymbol{J}}(\boldsymbol{q},\dot{\boldsymbol{q}})\dot{\boldsymbol{q}}\big) \tag{9.39}$$

where $\boldsymbol{x}_F$ is a suitable reference to be related to a force error. Notice that the control law (9.39) does not foresee the adoption of compensating actions relative to $\dot{\boldsymbol{x}}_F$ and $\ddot{\boldsymbol{x}}_F$. Moreover, since the operational space is defined only by position variables, the analytical Jacobian coincides with the geometric Jacobian and thus $\boldsymbol{J}_A(\boldsymbol{q}) = \boldsymbol{J}(\boldsymbol{q})$.

Substituting (9.30), (9.39) into (9.1), leads, after similar algebraic manipulation as above, to the system described by

$$\boldsymbol{M}_d\ddot{\boldsymbol{x}}_e + \boldsymbol{K}_D\dot{\boldsymbol{x}}_e + \boldsymbol{K}_P\boldsymbol{x}_e = \boldsymbol{K}_P\boldsymbol{x}_F, \tag{9.40}$$

which shows how (9.30) and (9.39) perform a position control taking $\boldsymbol{x}_e$ to $\boldsymbol{x}_F$ with a dynamics specified by the choice of matrices $\boldsymbol{M}_d$, $\boldsymbol{K}_D$, $\boldsymbol{K}_P$.

Let $\boldsymbol{f}_d$ denote the desired *constant* force reference; the relation between $\boldsymbol{x}_F$ and the force error can be expressed as

$$\boldsymbol{x}_F = \boldsymbol{C}_F(\boldsymbol{f}_d - \boldsymbol{f}_e), \tag{9.41}$$

where $\boldsymbol{C}_F$ is a diagonal matrix, with the meaning of compliance, whose elements give the control actions to perform along the operational space directions of interest. The equations in (9.40), (9.41) reveal that force control is developed on the basis of a preexisting position control loop.

On the assumption of the elastically compliant environment described by (9.38), the equation in (9.40) with (9.41) becomes

$$\boldsymbol{M}_d\ddot{\boldsymbol{x}}_e + \boldsymbol{K}_D\dot{\boldsymbol{x}}_e + \boldsymbol{K}_P(\boldsymbol{I}_3 + \boldsymbol{C}_F\boldsymbol{K})\boldsymbol{x}_e = \boldsymbol{K}_P\boldsymbol{C}_F(\boldsymbol{K}\boldsymbol{x}_r + \boldsymbol{f}_d). \tag{9.42}$$

To decide about the kind of control action to specify with $\boldsymbol{C}_F$, it is worth representing (9.21), (9.40), (9.41) in terms of the block scheme in Fig. 9.6,

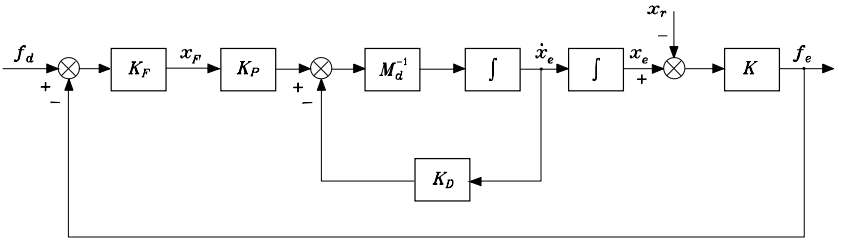

Fig. 9.7. Block scheme of force control with inner velocity loop

which is logically derived from the scheme in Fig. 9.3. This scheme suggests that if $\boldsymbol{C}_F$ has a purely proportional control action, then $\boldsymbol{f}_e$ cannot reach $\boldsymbol{f}_d$ and $\boldsymbol{x}_r$ influences the interaction force also at steady state.

If $\boldsymbol{C}_F$ also has an integral control action on the force components, then it is possible to achieve $\boldsymbol{f}_e = \boldsymbol{f}_d$ at steady state and, at the same time, to reject the effect of $\boldsymbol{x}_r$ on $\boldsymbol{f}_e$. Hence, a convenient choice for $\boldsymbol{C}_F$ is a *proportional-integral* (PI) *action*

$$\boldsymbol{C}_F = \boldsymbol{K}_F + \boldsymbol{K}_I \int^t (\cdot)\, d\varsigma. \tag{9.43}$$

The dynamic system resulting from (9.42), (9.43) is of third order, and then it is necessary to choose adequately the matrices $\boldsymbol{K}_D$, $\boldsymbol{K}_P$, $\boldsymbol{K}_F$, $\boldsymbol{K}_I$ in respect of the characteristics of the environment. Since the values of environment stiffness are typically high, the weight of the proportional and integral actions should be contained; the choice of $\boldsymbol{K}_F$ and $\boldsymbol{K}_I$ influences the stability margins and the bandwidth of the system under force control. On the assumption that a stable equilibrium is reached, it is $\boldsymbol{f}_e = \boldsymbol{f}_d$ and then

$$\boldsymbol{K}\boldsymbol{x}_e = \boldsymbol{K}\boldsymbol{x}_r + \boldsymbol{f}_d. \tag{9.44}$$

9.4.2 Force Control with Inner Velocity Loop

From the block scheme of Fig. 9.6 it can be observed that, if the position feedback loop is opened, $\boldsymbol{x}_F$ represents a velocity reference, and then an integration relationship exists between $\boldsymbol{x}_F$ and $\boldsymbol{x}_e$. This leads to recognizing that, in this case, the interaction force with the environment coincides with the desired value at steady state, even with a proportional force controller $\boldsymbol{C}_F$. In fact, choosing

$$\boldsymbol{y} = \boldsymbol{J}^{-1}(\boldsymbol{q})\boldsymbol{M}_d^{-1}\big(-\boldsymbol{K}_D\dot{\boldsymbol{x}}_e + \boldsymbol{K}_P\boldsymbol{x}_F - \boldsymbol{M}_d\dot{\boldsymbol{J}}(\boldsymbol{q},\dot{\boldsymbol{q}})\dot{\boldsymbol{q}}\big), \tag{9.45}$$

with a purely proportional control structure ($\boldsymbol{C}_F = \boldsymbol{K}_F$) on the force error yields

$$\boldsymbol{x}_F = \boldsymbol{K}_F(\boldsymbol{f}_d - \boldsymbol{f}_e) \tag{9.46}$$

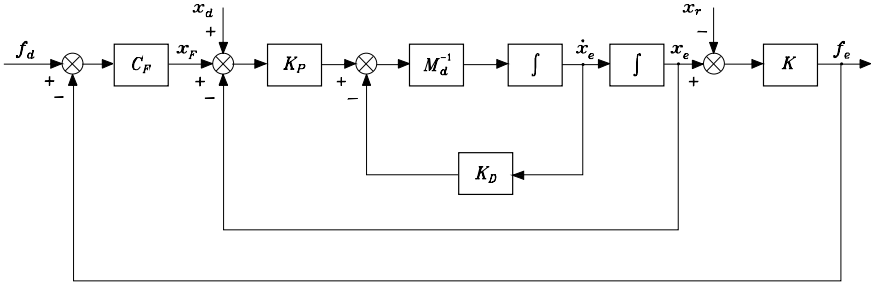

Fig. 9.8. Block scheme of parallel force/position control

and then system dynamics is described by

$$\boldsymbol{M}_d\ddot{\boldsymbol{x}}_e + \boldsymbol{K}_D\dot{\boldsymbol{x}}_e + \boldsymbol{K}_P\boldsymbol{K}_F\boldsymbol{K}\boldsymbol{x}_e = \boldsymbol{K}_P\boldsymbol{K}_F(\boldsymbol{K}\boldsymbol{x}_r + \boldsymbol{f}_d). \tag{9.47}$$

The relationship between position and contact force at the equilibrium is given by (9.44). The corresponding block scheme is reported in Fig. 9.7. It is worth emphasizing that control design is simplified, since the resulting system now is of second order;[2] it should be noticed, however, that the absence of an integral action in the force controller does not ensure reduction of the effects due to unmodelled dynamics.

9.4.3 Parallel Force/Position Control

The force control schemes presented require the force reference to be consistent with the geometric features of the environment. In fact, if $\boldsymbol{f}_d$ has components outside $\mathcal{R}(\boldsymbol{K})$, both (9.42) (in case of an integral action in $\boldsymbol{C}_F$) and (9.47) show that, along the corresponding operational space directions, the components of $\boldsymbol{f}_d$ are interpreted as velocity references which cause a drift of the end-effector position. If $\boldsymbol{f}_d$ is correctly planned along the directions outside $\mathcal{R}(\boldsymbol{K})$, the resulting motion governed by the position control action tends to take the end-effector position to zero in the case of (9.42), and the end-effector velocity to zero in the case of (9.47). Hence, the above control schemes do not allow position control even along the admissible task space directions.

If it is desired to specify a desired end-effector pose $\boldsymbol{x}_d$ as in pure position control schemes, the scheme of Fig. 9.6 can be modified by adding the reference $\boldsymbol{x}_d$ to the input where positions are summed. This corresponds to choosing

$$\boldsymbol{y} = \boldsymbol{J}^{-1}(\boldsymbol{q})\boldsymbol{M}_d^{-1}\big(-\boldsymbol{K}_D\dot{\boldsymbol{x}}_e + \boldsymbol{K}_P(\widetilde{\boldsymbol{x}} + \boldsymbol{x}_F) - \boldsymbol{M}_d\dot{\boldsymbol{J}}_A(\boldsymbol{q},\dot{\boldsymbol{q}})\dot{\boldsymbol{q}}\big) \tag{9.48}$$

where $\widetilde{\boldsymbol{x}} = \boldsymbol{x}_d - \boldsymbol{x}_e$. The resulting scheme (Fig. 9.8) is termed *parallel force/position control*, in view of the presence of a position control action

[2] The matrices $\boldsymbol{K}_P$ and $\boldsymbol{K}_F$ are not independent and one may refer to a single matrix $\boldsymbol{K}'_F = \boldsymbol{K}_P\boldsymbol{K}_F$.

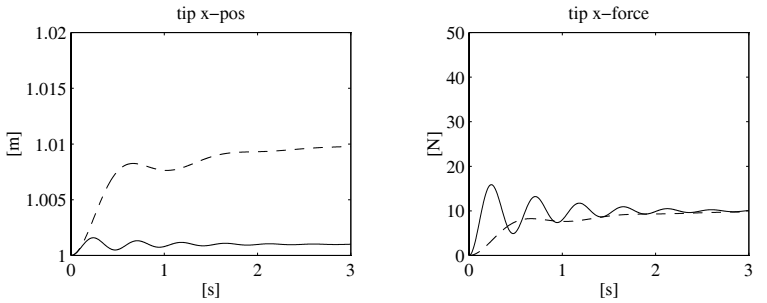

Fig. 9.9. Time history of the tip position and of the contact force along horizontal direction with force control scheme with inner position loop for two environments of different compliance

$\boldsymbol{K}_P\widetilde{\boldsymbol{x}}$ in parallel to a force control action $\boldsymbol{K}_P\boldsymbol{C}_F(\boldsymbol{f}_d - \boldsymbol{f}_e)$. It is easy to verify that, in this case, the equilibrium position satisfies the equation (see Problem 9.4)

$$\boldsymbol{x}_e = \boldsymbol{x}_d + \boldsymbol{C}_F\big(\boldsymbol{K}(\boldsymbol{x}_r - \boldsymbol{x}_e) + \boldsymbol{f}_d\big). \tag{9.49}$$

Therefore, along those directions outside $\mathcal{R}(\boldsymbol{K})$ where motion is unconstrained, the position reference $\boldsymbol{x}_d$ is reached by $\boldsymbol{x}_e$. Vice versa, along those directions in $\mathcal{R}(\boldsymbol{K})$ where motion is constrained, $\boldsymbol{x}_d$ is treated as an additional disturbance; the adoption of an integral action in $\boldsymbol{C}_F$ as for the scheme of Fig. 9.6 ensures that the force reference $\boldsymbol{f}_d$ is reached at steady state, at the expense of a position error on $\boldsymbol{x}_e$ depending on environment compliance.

Example 9.3

Consider again the planar arm in contact with the elastically compliant plane of the above examples; let the initial contact position be the same as that of Example 9.2. Performance of the various force control schemes is analyzed; as in Example 9.2, a more compliant ($k_x = 10^3$ N/m) and a less compliant ($k_x = 10^4$ N/m) environment are considered. The position control actions $\boldsymbol{M}_d$, $\boldsymbol{K}_D$, $\boldsymbol{K}_P$ are chosen as in Example 9.2; a force control action is added along the horizontal direction, namely

$$\boldsymbol{C}_F = \text{diag}\{c_{Fx}, 0\}.$$

The reference for the contact force is chosen as $\boldsymbol{f}_d = [\,10 \quad 0\,]^T$; the position reference — meaningful only for the parallel control — is taken as $\boldsymbol{x}_d = [\,1.015 \quad 0.1\,]^T$.

With regard to the scheme with inner position loop of Fig. 9.6, a PI control action c_{Fx} is chosen with parameters:

$$k_{Fx} = 0.00064 \qquad k_{Ix} = 0.0016.$$

This confers two complex poles $(-1.96, \pm j5.74)$, a real pole (-1.09), and a real zero (-2.5) to the overall system, for the more compliant environment.

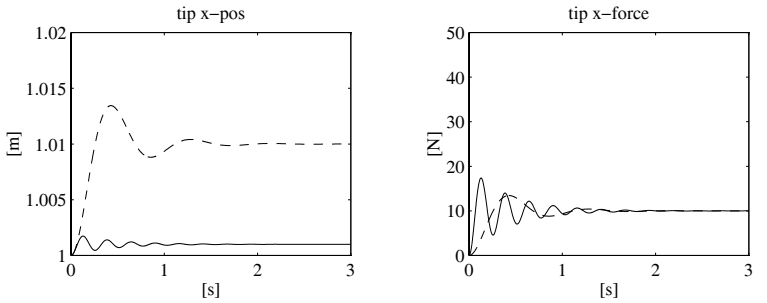

Fig. 9.10. Time history of the tip position and of the contact force along horizontal direction with force control scheme with inner velocity loop for two environments of different compliance

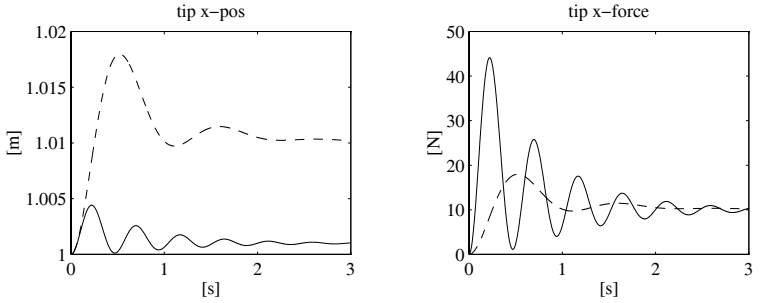

Fig. 9.11. Time history of tip position and of the contact force along horizontal direction with parallel force/position control scheme for two environments of different compliance

With regard to the scheme with inner velocity loop of Fig. 9.7, the proportional control action in c_{Fx} is

$$k_{Fx} = 0.0024$$

so that the overall system, for the more compliant environment, has two complex poles $(-2.5, \pm j7.34)$.

With regard to the parallel control scheme of Fig. 9.8, the PI control action c_{Fx} is chosen with the same parameters as for the first control scheme.

Figures 9.9, 9.10, 9.11 report the time history of the tip position and contact force along axis x_0 for the three considered schemes. A comparison between the various cases shows what follows:

- All control laws guarantee a steady-state value of contact forces equal to the desired one for both the more compliant (*dashed line*) and the less compliant (*continuous line*) environment.
- For given motion control actions ($\boldsymbol{M}_d$, $\boldsymbol{K}_D$, $\boldsymbol{K}_P$), the force control with inner velocity loop presents a faster dynamics than that of the force control with inner position loop.
- The dynamic response with the parallel control shows how the addition of a position reference along the horizontal direction degrades the transient behaviour,

but it does not influence the steady-state contact force. This effect can be justified by noting that a step position input is equivalent to a properly filtered impulse force input.

The reference position along axis y_0 is obviously reached by the arm tip according to dynamics of position control; the relative time history is not reported.

9.5 Constrained Motion

Force control schemes can be employed for the execution of a *constrained motion* as long as they suitably take into account the geometric features of the environment and the force and position references are chosen to be compatible with those features.

A real manipulation task is characterized by complex contact situations where some directions are subject to end-effector pose constraints and others are subject to interaction force constraints. During task execution, the nature of constraints may vary substantially.

The need to handle complex contact situations requires the capacity to specify and perform control of both end-effector pose and contact force. However, a fundamental aspect to be considered is that it is not possible to impose simultaneously arbitrary values of pose and force along each direction. Moreover, one should ensure that the reference trajectories for the control system be compatible with the constraints imposed by the environment during task execution.

For the above reasons, it is useful to have an analytical description of the interaction forces, which is very demanding from a modelling point of view.

A real contact situation is a naturally distributed phenomenon in which the local characteristics of the contact surfaces as well as the global dynamics of the manipulator and environment are involved. In detail:

- The environment imposes kinematic constraints on the end-effector motion, due to one or more contacts of different type; reaction forces and moments arise when the end-effector tends to violate the constraints (e.g., the case of a robot sliding a rigid tool on a frictionless rigid surface).
- The end-effector, while being subject to kinematic constraints, may also exert dynamic forces and moments on the environment, in the presence of environment dynamics (e.g., the case of a robot turning a crank, when the crank dynamics is relevant, or a robot pushing against a compliant surface).
- The contact force and moment may depend on the structural compliance of the robot, due to the finite stiffness of the joints and links of the manipulator, as well as of the wrist force/torque sensor or of the tool (e.g. an end-effector mounted on an RCC device).

- Local deformations of the contact surfaces may occur during the interaction, producing distributed contact areas; moreover, static and dynamic friction may be present in the case of non-ideally smooth contact surfaces.

The design of the interaction control is usually carried out under simplifying assumptions. The following two cases are considered:

- The robot and the environment are perfectly rigid and purely kinematics constraints are imposed by the environment.
- The robot is perfectly rigid, all the compliance of the system is localized in the environment and the contact force and moment is approximated by a linear elastic model.

In both cases, frictionless contact is assumed. It is obvious that these situations are only ideal. However, the robustness of the control should be able to cope with situations where some of the ideal assumptions are relaxed. In that case the control laws may be adapted to deal with non-ideal characteristics.

9.5.1 Rigid Environment

The kinematic constraints imposed by the environment can be represented by a set of algebraic equations that the variables describing the end-effector position and orientation must satisfy; since these variables depend on the joint variables through the direct kinematic equations, the constraint equations can also be expressed in the joint space as

$$\boldsymbol{\varphi}(\boldsymbol{q}) = \mathbf{0}. \tag{9.50}$$

Vector $\boldsymbol{\varphi}$ is an $(m \times 1)$ function, with $m < n$, where n is the number of joints of the manipulator, assumed to be nonredundant; without loss of generality, the case $n = 6$ is considered. The constraints of the form (9.50), involving only the generalized coordinates of the system, are known as *holonomic constraints*. Computing the time derivative of (9.50) yields

$$\boldsymbol{J}_{\varphi}(\boldsymbol{q})\dot{\boldsymbol{q}} = \mathbf{0}, \tag{9.51}$$

where $\boldsymbol{J}_{\varphi}(\boldsymbol{q}) = \partial\boldsymbol{\varphi}/\partial\boldsymbol{q}$ is the $(m \times 6)$ Jacobian of $\boldsymbol{\varphi}(\boldsymbol{q})$, known as *constraint Jacobian*. It is assumed that $\boldsymbol{J}_{\varphi}$ is of rank m at least locally in a neighborhood of the operating point; equivalently, the m constraint equations (9.50) are assumed to be locally independent.

In the absence of friction, the interaction forces are *reaction forces* arising when the end-effector tends to violate the constraints. These end-effector forces produce reaction torques at the joints that can be computed using the principle of virtual work, taking into account that the work of the reaction forces, by definition, should be null for all virtual displacements which satisfy the constraints. Considering the expression (3.108) of the virtual work of the

joint torques $\boldsymbol{\tau}$ and that, in view of (9.51), the virtual displacement $\delta\boldsymbol{q}$ satisfy the equation

$$\boldsymbol{J}_{\varphi}(\boldsymbol{q})\delta\boldsymbol{q} = \boldsymbol{0},$$

yields

$$\boldsymbol{\tau} = \boldsymbol{J}_{\varphi}^{T}(\boldsymbol{q})\boldsymbol{\lambda},$$

where $\boldsymbol{\lambda}$ is a suitable $(m \times 1)$ vector. The corresponding forces applied to the end-effector are

$$\boldsymbol{h}_e = \boldsymbol{J}^{-T}(\boldsymbol{q})\boldsymbol{\tau} = \boldsymbol{S}_f(\boldsymbol{q})\boldsymbol{\lambda}, \tag{9.52}$$

assuming a nonsingular $\boldsymbol{J}$, with

$$\boldsymbol{S}_f = \boldsymbol{J}^{-T}(\boldsymbol{q})\boldsymbol{J}_{\varphi}^{T}(\boldsymbol{q}). \tag{9.53}$$

Notice that Eq. (9.50) corresponds to a set of *bilateral constraints*. This means that the reaction forces (9.52) act so that, during the motion, the end-effector always keeps contact with the environment, as for the case of a gripper turning a crank. However, in many applications, the interaction with the environment corresponds to *unilateral constraints*. For example, in the case of a tool sliding on a surface, the reaction forces arise only when the tool pushes against the surface and not when it tends to detach. However, Eq. (9.52) can be still applied under the assumption that the end-effector, during the motion, never loses contact with the environment.

From (9.52) it follows that $\boldsymbol{h}_e$ belongs to the m-dimensional subspace $\mathcal{R}(\boldsymbol{S}_f)$. The inverse of the linear transformation (9.52) can be computed as

$$\boldsymbol{\lambda} = \boldsymbol{S}_f^{\dagger}(\boldsymbol{q})\boldsymbol{h}_e, \tag{9.54}$$

where $\boldsymbol{S}_f^{\dagger}$ denotes a weighted pseudo-inverse of matrix $\boldsymbol{S}_f$, namely

$$\boldsymbol{S}_f^{\dagger} = (\boldsymbol{S}_f^{T}\boldsymbol{W}\boldsymbol{S}_f)^{-1}\boldsymbol{S}_f^{T}\boldsymbol{W}, \tag{9.55}$$

where $\boldsymbol{W}$ is a symmetric and positive definite weighting matrix.

Notice that, while subspace $\mathcal{R}(\boldsymbol{S}_f)$ is uniquely defined by the geometry of the contact, matrix $\boldsymbol{S}_f$ in (9.53) is not unique, because constraint equations (9.50) are not uniquely defined. Moreover, in general, the physical dimensions of the elements of vector $\boldsymbol{\lambda}$ are not homogeneous and the columns of matrix $\boldsymbol{S}_f$, as well as of matrix $\boldsymbol{S}_f^{\dagger}$, do not necessarily represent homogeneous entities. This may produce invariance problems in the transformation (9.54) if $\boldsymbol{h}_e$ represents a quantity that is subject to disturbances and, as a result, may have components outside $\mathcal{R}(\boldsymbol{S}_f)$. In particular, if a physical unit or a reference frame is changed, matrix $\boldsymbol{S}_f$ undergoes a transformation; however, the result of (9.54) with the transformed pseudo-inverse, in general, depends on the adopted physical units or reference frame! The reason is that, if $\boldsymbol{h}_e \notin \mathcal{R}(\boldsymbol{S}_f)$, the problem of computing $\boldsymbol{\lambda}$ from (9.52) does not have a solution. In this case, Eq. (9.54) represents only an approximate solution which minimizes the norm

of vector $\boldsymbol{h}_e - \boldsymbol{S}_f(\boldsymbol{q})\boldsymbol{\lambda}$ weighted by matrix $\boldsymbol{W}$.[3] It is evident that the invariance of the solution can be ensured only if, in the case that a physical unit or a reference frame is changed, the weighting matrix is transformed accordingly. In the ideal case $\boldsymbol{h}_e \in \mathcal{R}(\boldsymbol{S}_f)$, the computation of the inverse of (9.52) has a unique solution, defined by (9.54), regardless the weighting matrix; hence the invariance problem does not occur.

In order to guarantee invariance, it is convenient choosing matrix $\boldsymbol{S}_f$ so that its columns represent linearly independent forces. This implies that (9.52) gives $\boldsymbol{h}_e$ as a linear combination of forces and $\boldsymbol{\lambda}$ is a dimensionless vector. Moreover, a physically consistent norm in the space of forces can be defined based on the quadratic form $\boldsymbol{h}_e^T \boldsymbol{C} \boldsymbol{h}_e$, which has the meaning of an elastic energy if $\boldsymbol{C}$ is a positive definite compliance matrix. Hence, the choice $\boldsymbol{W} = \boldsymbol{C}$ can be made for the weighting matrix and, if a physical unit or a reference frame is changed, the transformations to be applied to matrices $\boldsymbol{S}_f$ and $\boldsymbol{W}$ can be easily found on the basis of their physical meaning.

Notice that, for a given $\boldsymbol{S}_f$, the constraint Jacobian can be computed from (9.53) as $\boldsymbol{J}_\varphi(\boldsymbol{q}) = \boldsymbol{S}_f^T \boldsymbol{J}(\boldsymbol{q})$; moreover, if necessary, the constraint equations can be derived by integrating (9.51).

By using (3.4), (9.53), equality (9.51) can be rewritten in the form

$$\boldsymbol{J}_\varphi(\boldsymbol{q})\boldsymbol{J}^{-1}(\boldsymbol{q})\boldsymbol{J}(\boldsymbol{q})\dot{\boldsymbol{q}} = \boldsymbol{S}_f^T \boldsymbol{v}_e = \boldsymbol{0}, \tag{9.56}$$

which, by virtue of (9.52), is equivalent to

$$\boldsymbol{h}_e^T \boldsymbol{v}_e = 0. \tag{9.57}$$

Equation (9.57) represents the kinetostatic relationship, known as *reciprocity*, between the interaction force and moment $\boldsymbol{h}_e$ — belonging to the so-called *force controlled subspace* — which coincides with $\mathcal{R}(\boldsymbol{S}_f)$ and the end-effector linear and angular velocity $\boldsymbol{v}_e$ — belonging to the so-called *velocity controlled subspace*. The concept of reciprocity expresses the physical fact that, under the assumption of rigid and frictionless contact, the forces do not produce any work for all the end-effector displacements which satisfy the constraints. This concept is often confused with the concept of orthogonality, which is meaningless in this case because velocities and forces are non-homogeneous quantities belonging to different vector spaces.

Equations (9.56), (9.57) imply that the dimension of the velocity controlled subspace is $6-m$ whereas the dimension of the force controlled subspace is m; moreover, a $(6 \times (6-m))$ matrix $\boldsymbol{S}_v$ can be defined, which satisfies equation

$$\boldsymbol{S}_f^T(\boldsymbol{q})\boldsymbol{S}_v(\boldsymbol{q}) = \boldsymbol{O} \tag{9.58}$$

and such that $\mathcal{R}(\boldsymbol{S}_v)$ represents the velocity controlled subspace. Therefore:

$$\boldsymbol{v}_e = \boldsymbol{S}_v(\boldsymbol{q})\boldsymbol{\nu}, \tag{9.59}$$

[3] See Sect. A.7 for the computation of an approximate solution based on the left pseudo-inverse and Problem 9.5.

where $\boldsymbol{\nu}$ denotes a suitable $((6-m)\times 1)$ vector.

The inverse of the linear transformation (9.59) can be computed as

$$\boldsymbol{\nu} = \boldsymbol{S}_v^{\dagger}(\boldsymbol{q})\boldsymbol{v}_e, \tag{9.60}$$

where $\boldsymbol{S}_v^{\dagger}$ denotes a suitable weighted pseudo-inverse of matrix $\boldsymbol{S}_v$, computed as in (9.55). Notice that, as for the case of $\boldsymbol{S}_f$, although the subspace $\mathcal{R}(\boldsymbol{S}_v)$ is uniquely defined, the choice of matrix $\boldsymbol{S}_v$ itself is not unique. Moreover, about Eq. (9.60), invariance problems analogous to that considered for the case of (9.54) can be observed. In this case, it is convenient to select the matrix $\boldsymbol{S}_v$ so that its columns represent a set of independent velocities; moreover, for the computation of the pseudo-inverse, a norm in the space of velocities can be defined based on the kinetic energy of a rigid body or on the elastic energy expressed in terms of the stiffness matrix $\boldsymbol{K} = \boldsymbol{C}^{-1}$.

Matrix $\boldsymbol{S}_v$ may also have an interpretation in terms of Jacobian. In fact, due to the presence of m independent holonomic constraints (9.50), the configuration of a manipulator in contact with the environment can be locally described in terms of a $((6-m)\times 1)$ vector $\boldsymbol{r}$ of independent coordinates. From the implicit function theorem, this vector can be defined as

$$\boldsymbol{r} = \boldsymbol{\psi}(\boldsymbol{q}), \tag{9.61}$$

where $\boldsymbol{\psi}(\boldsymbol{q})$ is any $((6-m)\times 1)$ vector function such that the m components of $\boldsymbol{\phi}(\boldsymbol{q})$ and the $6-m$ components of $\boldsymbol{\psi}(\boldsymbol{q})$ are linearly independent at least locally in a neighborhood of the operating point. This means that the mapping (9.61), together with the constraint equations (9.50), is locally invertible, with inverse defined as

$$\boldsymbol{q} = \boldsymbol{\rho}(\boldsymbol{r}). \tag{9.62}$$

Equation (9.62) explicitly provides all the joint vectors $\boldsymbol{q}$ which satisfy the constraint equations (9.50), for any $\boldsymbol{r}$ arbitrary selected in a neighborhood of the operating point. Moreover, the vector $\dot{\boldsymbol{q}}$ that satisfies (9.51) can be computed as

$$\dot{\boldsymbol{q}} = \boldsymbol{J}_{\rho}(\boldsymbol{r})\dot{\boldsymbol{r}},$$

where $\boldsymbol{J}_{\rho}(\boldsymbol{r}) = \partial\boldsymbol{\rho}/\partial\boldsymbol{r}$ is a $(6\times(6-m))$ full rank Jacobian matrix. Also, the following equality holds:

$$\boldsymbol{J}_{\varphi}(\boldsymbol{q})\boldsymbol{J}_{\rho}(\boldsymbol{r}) = \boldsymbol{O},$$

which can be interpreted as a reciprocity condition between the subspace $\mathcal{R}(\boldsymbol{J}_{\varphi}^T)$ of the joint torques $\boldsymbol{\tau}$ corresponding to the reaction forces acting on the end-effector and the subspace $\mathcal{R}(\boldsymbol{J}_{\rho})$ of the joint velocities $\dot{\boldsymbol{q}}$ which satisfy the constraints.

The above equation can be rewritten as

$$\boldsymbol{J}_{\varphi}(\boldsymbol{q})\boldsymbol{J}^{-1}(\boldsymbol{q})\boldsymbol{J}(\boldsymbol{q})\boldsymbol{J}_{\rho}(\boldsymbol{r}) = \boldsymbol{O}.$$

Hence, assuming that $\boldsymbol{J}$ is nonsingular and taking into account (9.53), (9.58), matrix $\boldsymbol{S}_v$ can be computed as

$$\boldsymbol{S}_v = \boldsymbol{J}(\boldsymbol{q})\boldsymbol{J}_\rho(\boldsymbol{r}). \tag{9.63}$$

The matrices $\boldsymbol{S}_f$, $\boldsymbol{S}_v$ and the corresponding pseudo-inverse matrices $\boldsymbol{S}_f^\dagger$, $\boldsymbol{S}_v^\dagger$ are known as *selection matrices*. These matrices play a fundamental role for task specification, since they can be used to assign the desired end-effector motion and the interaction forces and moments consistently with the constraints. Also, they are essential for control synthesis.

To this end, notice that the (6×6) matrix $\boldsymbol{P}_f = \boldsymbol{S}_f \boldsymbol{S}_f^\dagger$ projects a generic force vector $\boldsymbol{h}_e$ on the force controlled subspace $\mathcal{R}(\boldsymbol{S}_f)$. Matrix $\boldsymbol{P}_f$ is idempotent, namely $\boldsymbol{P}_f^2 = \boldsymbol{P}_f \boldsymbol{P}_f = \boldsymbol{P}_f$, and therefore is a *projection matrix*. Moreover, matrix $(\boldsymbol{I}_6 - \boldsymbol{P}_f)$ projects force vector $\boldsymbol{h}_e$ on the orthogonal complement of the force controlled subspace; also, this matrix, being idempotent, it is a projection matrix.

Similarly, it can be verified that the (6×6) matrices $\boldsymbol{P}_v = \boldsymbol{S}_v \boldsymbol{S}_v^\dagger$ and $(\boldsymbol{I}_6 - \boldsymbol{P}_v)$ are projection matrices, projecting a generic linear and angular velocity vector $\boldsymbol{v}_e$ on the controlled velocity subspace $\mathcal{R}(\boldsymbol{S}_v)$ and on its orthogonal complement.

9.5.2 Compliant Environment

In many applications, the interaction forces between the end-effector and a compliant environment can be approximated by the ideal elastic model of the form (9.21). If the stiffness matrix $\boldsymbol{K}$ is positive definite, this model corresponds to a fully constrained case and the environment deformation coincides with the elementary end-effector displacement. In general, however, the end-effector motion is only partially constrained by the environment and this situation can be modelled by introducing a suitable positive semi-definite stiffness matrix.

This kind of situation, even for a simple case, has been already considered in previous examples concerning the interaction with an elastically compliant plane. In a general case, the stiffness matrix describing the partially constrained interaction can be computed by modelling the environment as a pair of rigid bodies, S and R, connected through an ideal six-DOF spring, and assuming that the end-effector may slide on the external surface of body S.

Moreover, two reference frames are introduced, one attached to S and one attached to R. At equilibrium, corresponding to the undeformed spring, the end-effector frame is assumed to be coincident with the frames attached to S and R. The selection matrices $\boldsymbol{S}_f$ and $\boldsymbol{S}_v$ and the corresponding controlled force and velocity subspaces can be identified on the basis of the geometry of the contact between the end-effector and the environment.

Assumed frictionless contact, the interaction force applied by the end-effector on body S belongs to the force controlled subspace $\mathcal{R}(\boldsymbol{S}_f)$ and thus

$$\boldsymbol{h}_e = \boldsymbol{S}_f \boldsymbol{\lambda}, \tag{9.64}$$

where $\boldsymbol{\lambda}$ is a $(m \times 1)$ vector. Due to the presence of the generalized spring, the above force causes a deformation of the environment that can be computed as

$$d\boldsymbol{x}_{r,s} = \boldsymbol{C}\boldsymbol{h}_e, \tag{9.65}$$

where $\boldsymbol{C}$ is the compliance matrix of the spring between S and R, assumed to be nonsingular. On the other hand, the elementary displacement of the end-effector with respect to the equilibrium pose can be decomposed as

$$d\boldsymbol{x}_{r,e} = d\boldsymbol{x}_v + d\boldsymbol{x}_f, \tag{9.66}$$

where

$$d\boldsymbol{x}_v = \boldsymbol{P}_v d\boldsymbol{x}_{r,e} \tag{9.67}$$

is the component belonging to the velocity controlled subspace $\mathcal{R}(\boldsymbol{S}_v)$, where the end-effector may slide on the environment, whereas

$$d\boldsymbol{x}_f = (\boldsymbol{I}_6 - \boldsymbol{P}_v) d\boldsymbol{x}_{r,e} = (\boldsymbol{I}_6 - \boldsymbol{P}_v) d\boldsymbol{x}_{r,s} \tag{9.68}$$

is the component corresponding to the deformation of the environment. Notice that, in general, $\boldsymbol{P}_v d\boldsymbol{x}_{r,e} \neq \boldsymbol{P}_v d\boldsymbol{x}_{r,s}$.

Premultiplying both sides of (9.66) by matrix $\boldsymbol{S}_f^T$ and using (9.67), (9.68), (9.65), (9.64) yields

$$\boldsymbol{S}_f^T d\boldsymbol{x}_{r,e} = \boldsymbol{S}_f^T d\boldsymbol{x}_{r,s} = \boldsymbol{S}_f^T \boldsymbol{C} \boldsymbol{S}_f \boldsymbol{\lambda},$$

where the equality $\boldsymbol{S}_f^T \boldsymbol{P}_v = \boldsymbol{O}$ has been taken into account. The above equation can be used to compute vector $\boldsymbol{\lambda}$ which, replaced into (9.64), yields

$$\boldsymbol{h}_e = \boldsymbol{K}' d\boldsymbol{x}_{r,e}, \tag{9.69}$$

where

$$\boldsymbol{K}' = \boldsymbol{S}_f (\boldsymbol{S}_f^T \boldsymbol{C} \boldsymbol{S}_f)^{-1} \boldsymbol{S}_f^T \tag{9.70}$$

is the positive semi-definite stiffness matrix corresponding to the partially constrained elastic interaction.

Expression (9.70) is not invertible. However, using Eqs. (9.68), (9.65), the following equality can be derived:

$$d\boldsymbol{x}_f = \boldsymbol{C}' \boldsymbol{h}_e, \tag{9.71}$$

where the matrix

$$\boldsymbol{C}' = (\boldsymbol{I}_6 - \boldsymbol{P}_v) \boldsymbol{C}, \tag{9.72}$$

of rank $6 - m$, has the meaning of compliance matrix.

Notice that contact between the manipulator and the environment may be compliant along some directions and rigid along other directions. Therefore, the force control subspace can be decomposed into two distinct subspaces, one corresponding to elastic forces and the other corresponding to reaction forces. Matrices $\boldsymbol{K}'$ and $\boldsymbol{C}'$ should be modified accordingly.

9.6 Natural and Artificial Constraints

An interaction task can be assigned in terms of a desired end-effector force $\boldsymbol{h}_d$ and velocity $\boldsymbol{v}_d$. In order to be consistent with the constraints, these vectors must lie in the force and velocity controlled subspaces respectively. This can be guaranteed by specifying vectors $\boldsymbol{\lambda}_d$ and $\boldsymbol{\nu}_d$ and computing $\boldsymbol{h}_d$ and $\boldsymbol{v}_d$ as

$$\boldsymbol{h}_d = \boldsymbol{S}_f \boldsymbol{\lambda}_d, \quad \boldsymbol{v}_d = \boldsymbol{S}_v \boldsymbol{\nu}_d,$$

where $\boldsymbol{S}_f$ and $\boldsymbol{S}_v$ have to be suitably defined on the basis of the geometry of the task. Therefore vectors $\boldsymbol{\lambda}_d$ and $\boldsymbol{\nu}_d$ will be termed 'desired force' and 'desired velocity' respectively.

For many robotic tasks it is possible to define an orthogonal reference frame, eventually time-varying, where the constraints imposed by the environment can be easily identified, making task specification direct and intuitive. This reference frame O_c–$x_c y_c z_c$ is known as *constraint frame*.

Two DOFs correspond to each axis of the constraint frame: one associated with the linear velocity or to the force along the axis direction and the other associated with the angular velocity and to the moment along the axis direction.

For a given constraint frame, in the case of rigid environment and absence of friction, it can be observed that:

- Along each DOF, the environment imposes to the manipulator's end-effector either a velocity constraint — in the sense that it does not allow translation along a direction or rotation about an axis — or a force constraint — in the sense that it does not allow the application of any force along a direction or any torque about an axis; such constraints are termed *natural constraints* since they are determined directly by task geometry.
- The manipulator can control only the variables which are not subject to natural constraints; the reference values for those variables are termed *artificial constraints* since they are imposed with regard to the strategy for executing the given task.

Notice that the two sets of constraints are complementary, in that they regard different variables for each DOF. Also, they allow a complete specification of the task, since they involve all variables.

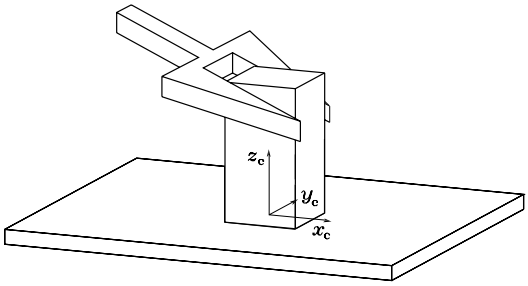

Fig. 9.12. Sliding of a prismatic object on a planar surface

In the case of compliant environment, for each DOF where interaction occurs, one can choose the variable to control, namely force or velocity, as long as the complementarity of the constraints is preserved. In case of high stiffness, it is advisable to choose the force as an artificial constraint and the velocity as a natural constraint, as for the case of rigid environment. Vice versa, in the case of low stiffness, it is convenient to make the opposite choice. Notice also that, in the presence of friction, forces and moments also arise along the DOFs corresponding to force natural constraints.

9.6.1 Analysis of Tasks

To illustrate description of an interaction task in terms of natural and artificial constraints as well as to emphasize the opportunity to use a constraint frame for task specification, in the following a number of typical case studies are analyzed.

Sliding on a planar surface

The end-effector manipulation task is the sliding of a prismatic object on a planar surface. Task geometry suggests choosing the constraint frame as attached to the contact plane with an axis orthogonal to the plane (Fig. 9.12). Alternatively, the task frame can be chosen with the same orientation but attached to the object.

Natural constraints can be determined first, assuming rigid and frictionless contact. Velocity constraints describe the impossibility to generate a linear velocity along axis z_c and angular velocities along axes x_c and y_c. Force constraints describe the impossibility to exert forces along axes x_c and y_c and a moment along axis z_c.

The artificial constraints regard the variables not subject to natural constraints. Hence, with reference to the natural constraints of force along axes x_c, y_c and moment along z_c, it is possible to specify artificial constraints for linear velocity along x_c, y_c and angular velocity along z_c. Similarly, with reference to natural constraints of linear velocity along axis z_c and angular velocity

about axes x_c and y_c, it is possible to specify artificial constraints for force along z_c and moments about x_c and y_c. The set of constraints is summarized in Table 9.1.

Table 9.1. Natural and artificial constraints for the task of Fig. 9.12

Natural constraints	Artificial constraints
$\dot{o}_z^c$	f_z^c
ω_x^c	μ_x^c
ω_y^c	μ_y^c
f_x^c	$\dot{o}_x^c$
f_y^c	$\dot{o}_y^c$
μ_z^c	ω_z^c

For this task, the dimension of the force controlled subspace is $m = 3$, while the dimension of the velocity controlled subspace is $6-m = 3$. Moreover, matrices $\boldsymbol{S}_f$ and $\boldsymbol{S}_v$ can be chosen as

$$\boldsymbol{S}_f = \begin{bmatrix} 0 & 0 & 0 \\ 0 & 0 & 0 \\ 1 & 0 & 0 \\ 0 & 1 & 0 \\ 0 & 0 & 1 \\ 0 & 0 & 0 \end{bmatrix} \qquad \boldsymbol{S}_v = \begin{bmatrix} 1 & 0 & 0 \\ 0 & 1 & 0 \\ 0 & 0 & 0 \\ 0 & 0 & 0 \\ 0 & 0 & 0 \\ 0 & 0 & 1 \end{bmatrix}.$$

Notice that, if the constraint frame is chosen attached to the contact plane, matrices $\boldsymbol{S}_f$ and $\boldsymbol{S}_v$ remain constant if referred to the base frame but are time-varying if referred to the end-effector frame. Vice versa, if the constraint frame is chosen attached to the object, such matrices are constant if referred to the end-effector frame and time-varying if referred to the base frame.

In the presence of friction, non-null force and moment may also arise along the velocity controlled DOFs.

In the case of compliant plane, elastic forces and torques may be applied along the axis z_c and about the axes x_c and y_c respectively, corresponding to end-effector displacements along the same DOFs. On the basis of the expressions derived for $\boldsymbol{S}_f$ and $\boldsymbol{S}_v$, the elements of the stiffness matrix $\boldsymbol{K}'$ corresponding to the partially constrained interaction are null with the exception of those of the (3×3) block $\boldsymbol{K}'_m$ obtained selecting the rows 3, 4 and 5 of $\boldsymbol{K}'$. This block matrix can be computed as

$$\boldsymbol{K}'_m = \begin{bmatrix} c_{3,3} & c_{3,4} & c_{3,5} \\ c_{4,3} & c_{4,4} & c_{4,5} \\ c_{5,3} & c_{5,4} & c_{5,5} \end{bmatrix}^{-1},$$

where $c_{i,j} = c_{j,i}$ are the elements of the (6×6) compliant matrix $\boldsymbol{C}$.

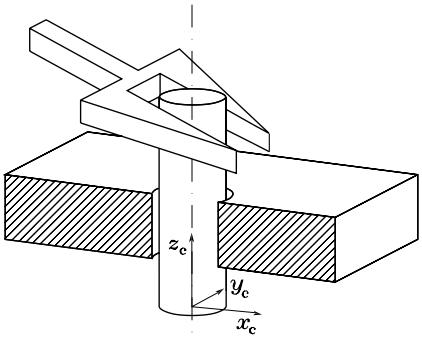

Fig. 9.13. Insertion of a cylindrical peg in a hole

Peg-in-hole

The end-effector manipulation task is the insertion of a cylindrical object (peg) in a hole. Task geometry suggests choosing the constraint frame with the origin in the centre of the hole and an axis parallel to the hole axis (Fig. 9.13). This frame can be chosen attached either to the peg or to the hole.

The natural constraints are determined by observing that it is not possible to generate arbitrary linear and angular velocities along axes x_c, y_c, nor is it possible to exert arbitrary force and moment along z_c. As a consequence, the artificial constraints can be used to specify forces and moments along x_c and y_c, as well as linear and angular velocity along z_c. Table 9.2 summarizes the constraints.

Table 9.2. Natural and artificial constraints for the task of Fig. 9.13

Natural constraints	Artificial constraints
$\dot{o}_x^c$	f_x^c
$\dot{o}_y^c$	f_y^c
ω_x^c	μ_x^c
ω_y^c	μ_y^c
f_z^c	$\dot{o}_z^c$
μ_z^c	ω_z^c

Among the variables subject to artificial constraints, $\dot{o}_z^c \neq 0$ describes insertion while the others are typically null to effectively perform the task.

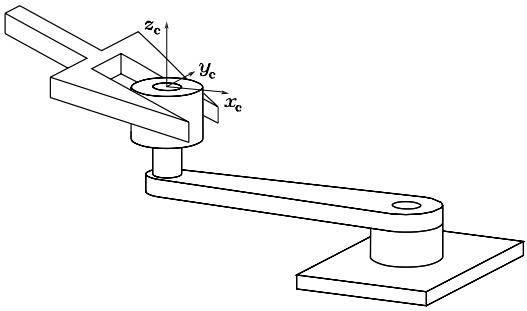

Fig. 9.14. Turning a crank

For this task, the dimension of the force controlled subspace is $m = 4$, while the dimension of the velocity controlled subspace is $6-m = 2$. Moreover, matrices $\boldsymbol{S}_f$ and $\boldsymbol{S}_v$ can be expressed as

$$\boldsymbol{S}_f = \begin{bmatrix} 1 & 0 & 0 & 0 \\ 0 & 1 & 0 & 0 \\ 0 & 0 & 0 & 0 \\ 0 & 0 & 1 & 0 \\ 0 & 0 & 0 & 1 \\ 0 & 0 & 0 & 0 \end{bmatrix} \qquad \boldsymbol{S}_v = \begin{bmatrix} 0 & 0 \\ 0 & 0 \\ 1 & 0 \\ 0 & 0 \\ 0 & 0 \\ 0 & 1 \end{bmatrix}.$$

Notice that, if the constraint frame is chosen attached to the hole, matrices $\boldsymbol{S}_f$ and $\boldsymbol{S}_v$ remain constant if referred to the base frame but are time-varying if referred to the end-effector frame. Vice versa, if the constraint frame is chosen attached to the peg, such matrices are constant if referred to the end-effector frame and time-varying if referred to the base frame.

Turning a crank

The end-effector manipulation task is the turning of a crank. Task geometry suggests choosing the constraint frame with an axis aligned with the axis of the idle handle and another axis aligned with the crank lever (Fig. 9.14). Notice that in this case the constraint frame is time-varying.

The natural constraints do not allow the generation of arbitrary linear velocities along x_c, z_c and angular velocities along x_c, y_c, nor arbitrary force along y_c and moment along z_c. As a consequence, the artificial constraints allow the specification of forces along x_c, z_c and moments along x_c, y_c, as well as a linear velocity along y_c and an angular velocity along z_c. The situation is summarized in Table 9.3.

Among the variables subject to artificial constraints, forces and moments are typically null for task execution.

Table 9.3. Natural and artificial constraints for task in Fig. 9.14

Natural constraints	Artificial constraints
$\dot{o}_x^c$	f_x^c
$\dot{o}_z^c$	f_z^c
ω_x^c	μ_x^c
ω_y^c	μ_y^c
f_y^c	$\dot{o}_y^c$
μ_z^c	ω_z^c

For this task, the dimension of the force controlled subspace is $m = 4$, while the dimension of the velocity controlled subspace is $6-m = 2$. Moreover, matrices $\boldsymbol{S}_f$ and $\boldsymbol{S}_v$ can be expressed as

$$\boldsymbol{S}_f = \begin{bmatrix} 1 & 0 & 0 & 0 \\ 0 & 0 & 0 & 0 \\ 0 & 1 & 0 & 0 \\ 0 & 0 & 1 & 0 \\ 0 & 0 & 0 & 1 \\ 0 & 0 & 0 & 0 \end{bmatrix} \qquad \boldsymbol{S}_v = \begin{bmatrix} 0 & 0 \\ 1 & 0 \\ 0 & 0 \\ 0 & 0 \\ 0 & 0 \\ 0 & 1 \end{bmatrix},$$

These matrices are constant in the constraint frame but are time-varying if referred to the base frame or to the end-effector frame, because the constraint frame moves with respect to both these frames during task execution.

9.7 Hybrid Force/Motion Control

Description of an interaction task between manipulator and environment in terms of natural constraints and artificial constraints, expressed with reference to the constraint frame, suggests a control structure that utilizes the artificial constraints to specify the objectives of the control system so that desired values can be imposed only onto those variables not subject to natural constraints. In fact, the control action should not affect those variables constrained by the environment so as to avoid conflicts between control and interaction with environment that may lead to an improper system behaviour. Such a control structure is termed *hybrid force/motion control*, since definition of artificial constraints involves both force and position or velocity variables.

For the design of hybrid control, it is useful rewriting the dynamic model of the manipulator with respect to the end-effector acceleration

$$\dot{\boldsymbol{v}}_e = \boldsymbol{J}(\boldsymbol{q})\ddot{\boldsymbol{q}} + \dot{\boldsymbol{J}}(\boldsymbol{q})\dot{\boldsymbol{q}}.$$

In particular, replacing (7.127) in the above expression yields

$$\boldsymbol{B}_e(\boldsymbol{q})\dot{\boldsymbol{v}}_e + \boldsymbol{n}_e(\boldsymbol{q}, \dot{\boldsymbol{q}}) = \boldsymbol{\gamma}_e - \boldsymbol{h}_e, \tag{9.73}$$

where

$$\boldsymbol{B}_e = \boldsymbol{J}^{-T}\boldsymbol{B}\boldsymbol{J}^{-1}$$
$$\boldsymbol{n}_e = \boldsymbol{J}^{-T}(\boldsymbol{C}\dot{\boldsymbol{q}} + \boldsymbol{g}) - \boldsymbol{B}_e\dot{\boldsymbol{J}}\dot{\boldsymbol{q}}.$$

In the following, hybrid force/motion control is presented first for the case of compliant environment and then for the case of rigid environment.

9.7.1 Compliant Environment

In the case of compliant environment, on the basis of the decomposition (9.66) and of Eqs. (9.67), (9.71), (9.64), the following expression can be found

$$d\boldsymbol{x}_{r,e} = \boldsymbol{P}_v d\boldsymbol{x}_{r,e} + \boldsymbol{C}'\boldsymbol{S}_f\boldsymbol{\lambda}.$$

Computing the elementary displacements in terms of velocity, in view of (9.59) and taking into account that frame r is motionless, the end-effector velocity can be decomposed as

$$\boldsymbol{v}_e = \boldsymbol{S}_v\boldsymbol{\nu} + \boldsymbol{C}'\boldsymbol{S}_f\dot{\boldsymbol{\lambda}}, \tag{9.74}$$

where the first term belongs to the velocity control subspace and the second term belongs to its orthogonal complement. All the quantities are assumed to be referred to a common reference frame which, for simplicity, was not specified.

In the following, the base frame is chosen as the common reference frame; moreover, the contact geometry and the compliance matrix are assumed to be constant, namely $\dot{\boldsymbol{S}}_v = \boldsymbol{O}$, $\dot{\boldsymbol{S}}_f = \boldsymbol{O}$ and $\dot{\boldsymbol{C}}' = \boldsymbol{O}$. Therefore, computing the time derivative of (9.74) yields the following decomposition for the end-effector acceleration:

$$\dot{\boldsymbol{v}}_e = \boldsymbol{S}_v\dot{\boldsymbol{\nu}} + \boldsymbol{C}'\boldsymbol{S}_f\ddot{\boldsymbol{\lambda}}. \tag{9.75}$$

By adopting the inverse dynamics control law

$$\boldsymbol{\gamma}_e = \boldsymbol{B}_e(\boldsymbol{q})\boldsymbol{\alpha} + \boldsymbol{n}_e(\boldsymbol{q}, \dot{\boldsymbol{q}}) + \boldsymbol{h}_e,$$

where $\boldsymbol{\alpha}$ is a new control input, in view of (9.73), the closed-loop equation is

$$\dot{\boldsymbol{v}}_e = \boldsymbol{\alpha}. \tag{9.76}$$

On the basis of the decomposition (9.75), with the choice

$$\boldsymbol{\alpha} = \boldsymbol{S}_v\boldsymbol{\alpha}_\nu + \boldsymbol{C}'\boldsymbol{S}_f\boldsymbol{f}_\lambda, \tag{9.77}$$

a complete decoupling between force control and velocity control can be achieved. In fact, replacing (9.75) and (9.77) into (9.76) and premultiplying both sides of the resulting equation once by $\boldsymbol{S}_v^\dagger$ and once by $\boldsymbol{S}_f^T$, the following equalities are obtained:

$$\dot{\boldsymbol{\nu}} = \boldsymbol{\alpha}_\nu \tag{9.78}$$
$$\ddot{\boldsymbol{\lambda}} = \boldsymbol{f}_\lambda. \tag{9.79}$$

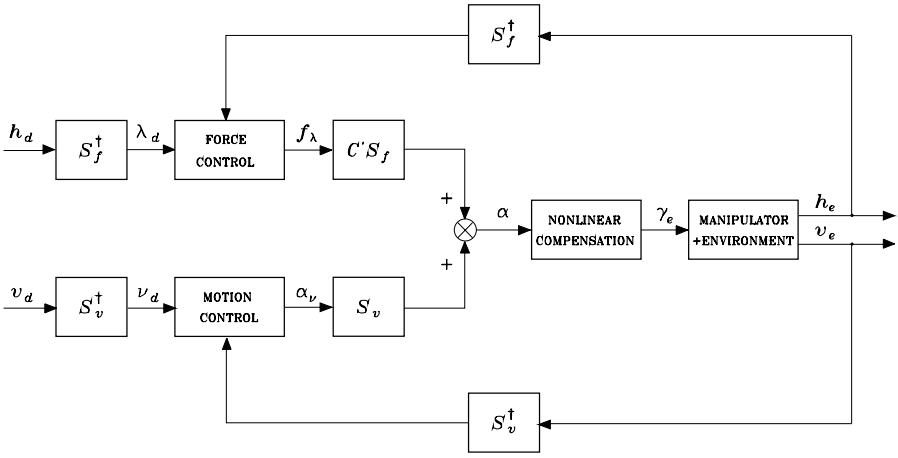

Fig. 9.15. Block scheme of a hybrid force/motion control for a compliant environment

Therefore, the task can be assigned specifying a desired force, in terms of vector $\boldsymbol{\lambda}_d(t)$, and a desired velocity, in terms of vector $\boldsymbol{\nu}_d(t)$. This control scheme is referred to as *hybrid force/velocity control*.

The desired velocity $\boldsymbol{\nu}_d$ can be achieved using the control law

$$\boldsymbol{\alpha}_\nu = \dot{\boldsymbol{\nu}}_d + \boldsymbol{K}_{P\nu}(\boldsymbol{\nu}_d - \boldsymbol{\nu}) + \boldsymbol{K}_{I\nu}\int_0^t (\boldsymbol{\nu}_d(\varsigma) - \boldsymbol{\nu}(\varsigma))\boldsymbol{d}\varsigma, \tag{9.80}$$

where $\boldsymbol{K}_{P\nu}$ and $\boldsymbol{K}_{I\nu}$ are positive definite matrices. Vector $\boldsymbol{\nu}$ can be computed using (9.60), where the linear and angular velocity of the end-effector $\boldsymbol{v}_e$ is computed from joint position and velocity measurements.

The desired force $\boldsymbol{\lambda}_d$ can be achieved using the control law

$$\boldsymbol{f}_\lambda = \ddot{\boldsymbol{\lambda}}_d + \boldsymbol{K}_{D\lambda}(\dot{\boldsymbol{\lambda}}_d - \dot{\boldsymbol{\lambda}}) + \boldsymbol{K}_{P\lambda}(\boldsymbol{\lambda}_d - \boldsymbol{\lambda}), \tag{9.81}$$

where $\boldsymbol{K}_{D\lambda}$ and $\boldsymbol{K}_{P\lambda}$ are positive definite matrices. The implementation of the above control law requires the computation of vector $\boldsymbol{\lambda}$ via (9.54), using the measurements of end-effector forces and moments $\boldsymbol{h}_e$. Also, $\dot{\boldsymbol{\lambda}}$ can be computed as

$$\dot{\boldsymbol{\lambda}} = \boldsymbol{S}_f^\dagger \dot{\boldsymbol{h}}_e$$

in the ideal case that $\dot{\boldsymbol{h}}_e$ is available.

The block scheme of a hybrid force/motion control law is shown in Fig. 9.15. The output variables are assumed to be the vector of end-effector forces and moments $\boldsymbol{h}_e$ and the vector of end-effector linear and angular velocities $\boldsymbol{v}_e$.

Since force measurements are often noisy, the use of $\dot{\boldsymbol{h}}_e$ is not feasible. Hence, the feedback of $\dot{\boldsymbol{\lambda}}$ is often replaced by

$$\dot{\boldsymbol{\lambda}} = \boldsymbol{S}_f^{\dagger} \boldsymbol{K}' \boldsymbol{J}(\boldsymbol{q}) \dot{\boldsymbol{q}}, \tag{9.82}$$

where $\boldsymbol{K}'$ is the positive semi-definite stiffness matrix (9.70).

If the contact geometry is known, but only an estimate of the stiffness/compliance of the environment is available, control law (9.77) can be rewritten in the form

$$\boldsymbol{\alpha} = \boldsymbol{S}_v \boldsymbol{\alpha}_\nu + \widehat{\boldsymbol{C}}' \boldsymbol{S}_f \boldsymbol{f}_\lambda,$$

where $\widehat{\boldsymbol{C}}' = (\boldsymbol{I}_6 - \boldsymbol{P}_v)\widehat{\boldsymbol{C}}$ and $\widehat{\boldsymbol{C}}$ is an estimate of $\boldsymbol{C}$.

In this case, Eq. (9.78) still holds while, in place of (9.79), the following equality can be derived:

$$\ddot{\boldsymbol{\lambda}} = \boldsymbol{L}_f \boldsymbol{f}_\lambda$$

where $\boldsymbol{L}_f = (\boldsymbol{S}_f^T \boldsymbol{C} \boldsymbol{S}_f)^{-1} \boldsymbol{S}_f^T \widehat{\boldsymbol{C}} \boldsymbol{S}_f$ is a nonsingular matrix. This implies that the force and velocity control subspaces remain decoupled and thus velocity control law (9.80) does not need to be modified.

Since matrix $\boldsymbol{L}_f$ is unknown, it is not possible to achieve the same performance of the force control as in the previous case. Also, if vector $\dot{\boldsymbol{\lambda}}$ is computed starting from velocity measurements using (9.82) with an estimate of $\boldsymbol{K}'$, only an estimate $\dot{\hat{\boldsymbol{\lambda}}}$ is available that, in view of (9.82), (9.70), can be expressed in the form

$$\dot{\hat{\boldsymbol{\lambda}}} = (\boldsymbol{S}_f^T \widehat{\boldsymbol{C}} \boldsymbol{S}_f)^{-1} \boldsymbol{S}_f^T \boldsymbol{J}(\boldsymbol{q}) \dot{\boldsymbol{q}}.$$

Replacing (9.74) in the above equation and using (9.72) yields

$$\dot{\hat{\boldsymbol{\lambda}}} = \boldsymbol{L}_f^{-1} \dot{\boldsymbol{\lambda}}. \tag{9.83}$$

Considering the control law

$$\boldsymbol{f}_\lambda = -k_{D\lambda} \dot{\hat{\boldsymbol{\lambda}}} + \boldsymbol{K}_{P\lambda}(\boldsymbol{\lambda}_d - \boldsymbol{\lambda}), \tag{9.84}$$

with a constant $\boldsymbol{\lambda}_d$, the dynamics of the closed-loop system is

$$\ddot{\boldsymbol{\lambda}} + k_{D\lambda} \dot{\boldsymbol{\lambda}} + \boldsymbol{L}_f \boldsymbol{K}_{P\lambda} \boldsymbol{\lambda} = \boldsymbol{L}_f \boldsymbol{K}_{P\lambda} \boldsymbol{\lambda}_d,$$

where expression (9.83) has been used. This equation shows that the equilibrium solution $\boldsymbol{\lambda} = \boldsymbol{\lambda}_d$ is also asymptotically stable in the presence of an uncertain matrix $\boldsymbol{L}_f$, with a suitable choice of gain $k_{D\lambda}$ and of matrix $\boldsymbol{K}_{P\lambda}$.

Example 9.4

Consider a two-link planar arm in contact with a purely frictionless elastic plane; unlike the above examples, the plane is at an angle of $\pi/4$ with axis x_0 (Fig. 9.16).

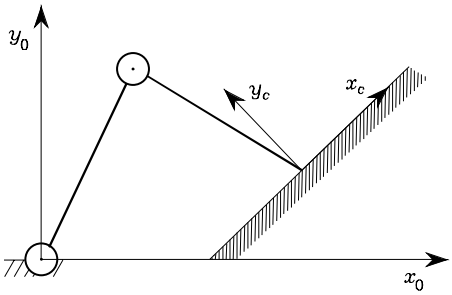

Fig. 9.16. Characterization of constraint frame for a two-link planar arm in contact with an elastically compliant plane

The natural choice of the constraint frame is that with axis x_c along the plane and axis y_c orthogonal to the plane; the task is obviously characterized by two DOFs. For the computation of the analytical model of the contact force, reference frames s and r are chosen so that, in the case of null force, they coincide with the constraint frame. In the presence of interaction, frame r remains attached to the rest position of the plane while frame s remains attached to the contact plane in the deformed position; the constraint frame is assumed to be attached to frame s. Matrices $\boldsymbol{S}_f^c$ and $\boldsymbol{S}_v^c$, referred to the constraint frame, have the form

$$\boldsymbol{S}_f^c = \begin{bmatrix} 0 \\ 1 \end{bmatrix} \quad \boldsymbol{S}_v^c = \begin{bmatrix} 1 \\ 0 \end{bmatrix},$$

and the corresponding projection matrices are

$$\boldsymbol{P}_f^c = \begin{bmatrix} 0 & 0 \\ 0 & 1 \end{bmatrix} \quad \boldsymbol{P}_v^c = \begin{bmatrix} 1 & 0 \\ 0 & 0 \end{bmatrix}.$$

In view of (9.70), (9.72), the stiffness and the compliance matrices, referred to the constraint frame, have the expression

$$\boldsymbol{K}'^c = \begin{bmatrix} 0 & 0 \\ 0 & c_{2,2}^{-1} \end{bmatrix} \quad \boldsymbol{C}'^c = \begin{bmatrix} 0 & 0 \\ 0 & c_{2,2} \end{bmatrix},$$

where $c_{2,2}$ characterizes the compliance of frame s with respect to frame r along the direction orthogonal to the plane, aligned to axis y_c of the constraint frame.

It is evident that, under the assumption that the plane is compliant only along the orthogonal direction and that this direction remains fixed, then the constraint frame orientation remains constant with respect to the base frame. The corresponding rotation matrix is given by

$$\boldsymbol{R}_c = \begin{bmatrix} 1/\sqrt{2} & -1/\sqrt{2} \\ 1/\sqrt{2} & 1/\sqrt{2} \end{bmatrix}. \tag{9.85}$$

Moreover, if the task is to slide the manipulator tip along the plane, the end-effector velocity can be decomposed according to (9.74) in the form

$$\boldsymbol{v}_e^c = \boldsymbol{S}_v^c \nu + \boldsymbol{C}'^c \boldsymbol{S}_f^c \dot{\lambda}, \tag{9.86}$$

where all the quantities are referred to the constraint frame. It can be easily shown that, if $\boldsymbol{f}_e^c = [\, f_x^c \quad f_y^c \,]^T$ and $\boldsymbol{v}_e^c = [\, \dot{o}_x^c \quad \dot{o}_y^c \,]^T$, it is $\nu = \dot{o}_x^c$ and $\lambda = f_y^c$. This equation can also be referred to the base frame, where matrices

$$\boldsymbol{S}_f = \boldsymbol{R}_c \boldsymbol{S}_f^c = \begin{bmatrix} -1/\sqrt{2} \\ 1/\sqrt{2} \end{bmatrix} \quad \boldsymbol{S}_v = \boldsymbol{R}_c \boldsymbol{S}_v^c = \begin{bmatrix} 1/\sqrt{2} \\ 1/\sqrt{2} \end{bmatrix},$$

are constant and the compliance matrix

$$\boldsymbol{C}' = \boldsymbol{R}_c \boldsymbol{C}'^c \boldsymbol{R}_c^T = c_{2,2} \begin{bmatrix} 1/2 & -1/2 \\ -1/2 & 1/2 \end{bmatrix}$$

is constant during the end-effector motion on the plane, for constant $c_{2,2}$. The adoption of an inverse dynamics control law, with the choice (9.77), leads to

$$\begin{aligned} \dot{\nu} &= \ddot{o}_x^c = \alpha_\nu \\ \ddot{\lambda} &= \ddot{f}_y^c = f_\lambda, \end{aligned}$$

showing that hybrid control achieves motion control along axis x_c and force control along axis y_c, provided that α_ν and f_λ are set according to (9.80) and (9.81) respectively.

Finally, notice that the formulation of the control law can be further simplified if the base frame is chosen parallel to the constraint frame.

9.7.2 Rigid Environment

In the case of rigid environment, the interaction force and moment can be written in the form $\boldsymbol{h}_e = \boldsymbol{S}_f \boldsymbol{\lambda}$. Vector $\boldsymbol{\lambda}$ can be eliminated from (9.73) by solving (9.73) for $\dot{\boldsymbol{v}}_e$ and substituting it into the time derivative of the equality (9.56). This yields

$$\boldsymbol{\lambda} = \boldsymbol{B}_f(\boldsymbol{q}) \Big(\boldsymbol{S}_f^T \boldsymbol{B}_e^{-1}(\boldsymbol{q})(\boldsymbol{\gamma}_e - \boldsymbol{n}_e(\boldsymbol{q}, \dot{\boldsymbol{q}})) + \dot{\boldsymbol{S}}_f^T \boldsymbol{v}_e \Big), \tag{9.87}$$

where $\boldsymbol{B}_f = (\boldsymbol{S}_f^T \boldsymbol{B}_e^{-1} \boldsymbol{S}_f)^{-1}$.

Hence, the dynamic model (9.73) for the manipulator constrained by the rigid environment can be rewritten in the form

$$\boldsymbol{B}_e(\boldsymbol{q})\dot{\boldsymbol{v}}_e + \boldsymbol{S}_f \boldsymbol{B}_f(\boldsymbol{q}) \dot{\boldsymbol{S}}_f^T \boldsymbol{v}_e = \boldsymbol{P}(\boldsymbol{q})(\boldsymbol{\gamma}_e - \boldsymbol{n}_e(\boldsymbol{q}, \dot{\boldsymbol{q}})), \tag{9.88}$$

with $\boldsymbol{P} = \boldsymbol{I}_6 - \boldsymbol{S}_f \boldsymbol{B}_f \boldsymbol{S}_f^T \boldsymbol{B}_e^{-1}$. Notice that $\boldsymbol{P}\boldsymbol{S}_f = \boldsymbol{O}$; moreover, this matrix is idempotent. Therefore, matrix $\boldsymbol{P}$ is a (6×6) projection matrix that filters out all the components of the end-effector forces lying in the subspace $\mathcal{R}(\boldsymbol{S}_f)$.

Equation (9.87) reveals that vector $\boldsymbol{\lambda}$ instantaneously depends on the control force $\boldsymbol{\gamma}_e$. Hence, by suitably choosing $\boldsymbol{\gamma}_e$, it is possible to control directly the m independent components of the end-effector forces that tend to violate the constraints; these components can be computed from $\boldsymbol{\lambda}$, using (9.52).

On the other hand, (9.88) represents a set of six second order differential equations whose solution, if initialized on the constraints, automatically satisfies Eq. (9.50) at all times.

The *reduced-order* dynamic model of the constrained system is described by $6 - m$ independent equations that are obtained premultiplying both sides of (9.88) by matrix $\boldsymbol{S}_v^T$ and substituting the acceleration $\dot{\boldsymbol{v}}_e$ with

$$\dot{\boldsymbol{v}}_e = \boldsymbol{S}_v \dot{\boldsymbol{\nu}} + \dot{\boldsymbol{S}}_v \boldsymbol{\nu}.$$

Using the identities (9.58) and $\boldsymbol{S}_v^T \boldsymbol{P} = \boldsymbol{S}_v^T$ yields

$$\boldsymbol{B}_v(\boldsymbol{q})\dot{\boldsymbol{\nu}} = \boldsymbol{S}_v^T \left(\boldsymbol{\gamma}_e - \boldsymbol{n}_e(\boldsymbol{q}, \dot{\boldsymbol{q}}) - \boldsymbol{B}_e(\boldsymbol{q})\dot{\boldsymbol{S}}_v \boldsymbol{\nu} \right), \tag{9.89}$$

where $\boldsymbol{B}_v = \boldsymbol{S}_v^T \boldsymbol{B}_e \boldsymbol{S}_v$. Moreover, expression (9.87) can be rewritten as

$$\boldsymbol{\lambda} = \boldsymbol{B}_f(\boldsymbol{q}) \boldsymbol{S}_f^T \boldsymbol{B}_e^{-1}(\boldsymbol{q}) \left(\boldsymbol{\gamma}_e - \boldsymbol{n}_e(\boldsymbol{q}, \dot{\boldsymbol{q}}) - \boldsymbol{B}_e(\boldsymbol{q})\dot{\boldsymbol{S}}_v \boldsymbol{\nu} \right), \tag{9.90}$$

where the identity $\dot{\boldsymbol{S}}_f^T \boldsymbol{S}_v = -\boldsymbol{S}_f^T \dot{\boldsymbol{S}}_v$ has been exploited.

With reference to (9.89), consider the choice

$$\boldsymbol{\gamma}_e = \boldsymbol{B}_e(\boldsymbol{q}) \boldsymbol{S}_v \boldsymbol{\alpha}_v + \boldsymbol{S}_f \boldsymbol{f}_\lambda + \boldsymbol{n}_e(\boldsymbol{q}, \dot{\boldsymbol{q}}) + \boldsymbol{B}_e(\boldsymbol{q}) \dot{\boldsymbol{S}}_v \boldsymbol{\nu}, \tag{9.91}$$

where $\boldsymbol{\alpha}_v$ and $\boldsymbol{f}_\lambda$ are new control inputs. By replacing (9.91) in (9.89), (9.90), the following two equations can be found:

$$\dot{\boldsymbol{\nu}} = \boldsymbol{\alpha}_\nu$$
$$\boldsymbol{\lambda} = \boldsymbol{f}_\lambda,$$

showing that the inverse dynamics control law (9.91) allows a complete decoupling between force and velocity controlled subspaces.

It is worth noticing that, for the implementation of control law (9.91), constraint equations (9.50) as well as Eq. (9.61) defining the vector of the configuration variables for the constrained system are not required, provided that matrices $\boldsymbol{S}_f$ and $\boldsymbol{S}_v$ are known. These matrices can be computed on the basis of the geometry of the environment or estimated on-line, using force and velocity measurements.

The task can easily be assigned by specifying a desired force, in terms of vector $\boldsymbol{\lambda}_d(t)$, and a desired velocity, in terms of vector $\boldsymbol{\nu}_d(t)$; the resulting scheme of *hybrid force/velocity control* is conceptually analogous to that shown in Fig. 9.15.

The desired velocity $\boldsymbol{\nu}_d$ can be achieved by setting $\boldsymbol{\alpha}_\nu$ according to (9.80), as for the case of compliant environment.

The desired force $\boldsymbol{\lambda}_d$ can be achieved by setting

$$\boldsymbol{f}_\lambda = \boldsymbol{\lambda}_d, \tag{9.92}$$

but this choice is very sensitive to disturbance forces, since it contains no force feedback. Alternative choices are

$$\boldsymbol{f}_\lambda = \boldsymbol{\lambda}_d + \boldsymbol{K}_{P\lambda}(\boldsymbol{\lambda}_d - \boldsymbol{\lambda}), \tag{9.93}$$

or

$$\boldsymbol{f}_\lambda = \boldsymbol{\lambda}_d + \boldsymbol{K}_{I\lambda}\int_0^t (\boldsymbol{\lambda}_d(\varsigma) - \boldsymbol{\lambda}(\varsigma))\boldsymbol{d}\varsigma, \tag{9.94}$$

where $\boldsymbol{K}_{P\lambda}$ and $\boldsymbol{K}_{I\lambda}$ are suitable positive definite matrices. The proportional feedback is able to reduce the force error due to disturbance forces, while the integral action is able to compensate for constant bias disturbances.

The implementation of force feedback requires the computation of vector $\boldsymbol{\lambda}$ from the measurement of the end-effector force and moment $\boldsymbol{h}_e$, that can be achieved using (9.54).

When Eqs. (9.50) and (9.61) are available, matrices $\boldsymbol{S}_f$ and $\boldsymbol{S}_v$ can be computed according to (9.53) and (9.63), respectively. Moreover, a *hybrid force/position control* can be designed specifying a desired force $\boldsymbol{\lambda}_d(t)$, and a desired position $\boldsymbol{r}_d(t)$.

The force control law can be designed as above, while the desired position $\boldsymbol{r}_d$ can be achieved with the choice (see Problem 9.11)

$$\boldsymbol{\alpha}_\nu = \ddot{\boldsymbol{r}}_d + \boldsymbol{K}_{Dr}(\dot{\boldsymbol{r}}_d - \boldsymbol{\nu}) + \boldsymbol{K}_{Pr}(\boldsymbol{r}_d - \boldsymbol{r}), \tag{9.95}$$

where $\boldsymbol{K}_{Dr}$ and $\boldsymbol{K}_{Pr}$ are suitable positive definite matrices. Vector $\boldsymbol{r}$ can be computed from the joint position measurements using (9.61).

Bibliography

Scientific publications on force control are numerous and cover a time period of about 30 years. Review papers are [243] for the first decade, and [63] for the second decade. Recent monographs on this subject are [90, 209].

Control based on the concept of compliance was originally proposed by [165] in the joint space and [190] in the Cartesian space. The Remote Centre of Compliance concept is presented in [55] and its use for assembling operation is discussed in [242]. A reference paper for modelling of six-DOF elastic systems is [136] and their properties are analyzed in [177, 74]. The idea of impedance control was presented in [95] and a similar formulation can be found in [105]. Various schemes of impedance based on different representations of the orientation error are presented in [31, 32] and a rigorous analysis can be found in [223].

Early works on force control are described in [241]. Approaches not requiring the exact knowledge of the environment model are force control with position feedforward [65] and parallel force/position control [40, 43].

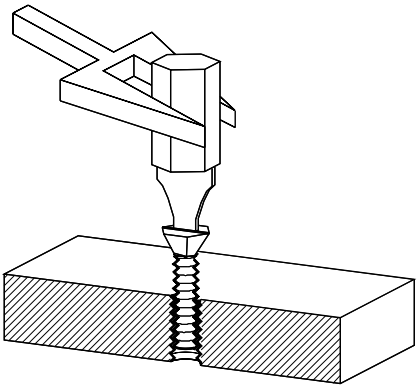

Fig. 9.17. Driving a screw in a hole

Natural and artificial constraints were introduced in [150] and further developed in [64, 27]. The concept of reciprocity of forces and velocity is discussed in [133], while invariance problems are analyzed in [66]. Models of elastic systems with semi-definite stiffness and compliance matrices are presented in [176]. The concept of hybrid force/motion control was introduced in [184] and the explicit inclusion of the manipulator dynamic model is presented in [114]. In [57] a systematic approach to modelling and control of interaction in the case of dynamic environment is introduced. Hybrid control in the presence of constraints in the Cartesian space is presented in [247, 249], while in [152] the constraints are formulated in the joint space. The use of impedance control in a hybrid framework is discussed in [5].

Adaptive versions of force/motion control schemes are proposed in [235]. The case of complex contact situations and time-varying constraints is presented in [28]. In [228, 62] the issues of controlling contact transitions is discussed, in order to overcome the instability problems evidenced in [70].

Problems

9.1. Derive expressions (9.10), (9.11).

9.2. Show that the equilibrium equations for the compliance control scheme are expressed by (9.22), (9.23).

9.3. Consider the planar arm in contact with the elastically compliant plane in Fig. 9.16. The plane forms an angle of $\pi/4$ with axis x_0 and its undeformed position intersects axis x_0 in the point of coordinates $(1, 0)$; the environment stiffness along axis y_c is $5 \cdot 10^3$ N/m. With the data of the arm in Sect. 8.7, design an impedance control. Perform a computer simulation of the interaction of the controlled manipulator along the rectilinear path from position $\boldsymbol{p}_i =$

$[\,1 \quad 0\,]^T$ to $\boldsymbol{p}_f = [\,1.2 + 0.1\sqrt{2} \quad 0.2\,]^T$ with a trapezoidal velocity profile and a trajectory duration $t_f = 1\,\text{s}$. Implement the control in discrete-time with a sampling time of 1 ms.

9.4. Show that the equilibrium position for the parallel force/position control scheme satisfies (9.49).

9.5. Show that expression (9.54) with (9.55) is the solution which minimizes the norm $\|\boldsymbol{h}_e - \boldsymbol{S}_f(\boldsymbol{q})\boldsymbol{\lambda}\|$ with weighting matrix $\boldsymbol{W}$.

9.6. Show that stiffness matrix (9.70) can be expressed in the form $\boldsymbol{K}' = \boldsymbol{P}_f\boldsymbol{K}$.

9.7. For the manipulation task of driving a screw in a hole illustrated in Fig. 9.17, find the natural constraints and artificial constraints with respect to a suitably chosen constraint frame.

9.8. Show that the hybrid control scheme of Example 9.4, in the force controlled subspace, is equivalent to a force control scheme with inner velocity loop.

9.9. For the arm and environment of Example 9.4 compute the expressions of $\boldsymbol{S}_f^\dagger$ and $\boldsymbol{S}_v^\dagger$ in the constraint frame and in the base frame.

9.10. For the arm and environment of Problem 9.3, design a hybrid control in which a motion control law operates along axis x_c while a force control law operates along axis y_c; let the desired contact force along axis y_c be 50 N. Perform a computer simulation of the interaction of the controlled manipulator along a trajectory on the plane equivalent to that of Problem 9.3. Implement the control in discrete-time with a sampling time of 1 ms.

9.11. Show that control law (9.95) ensures tracking of a desired position $\boldsymbol{r}_d(t)$.